Cell Reports

Article

# Increased replication origin firing links replication stress to whole chromosomal instability in human cancer

## Graphical abstract

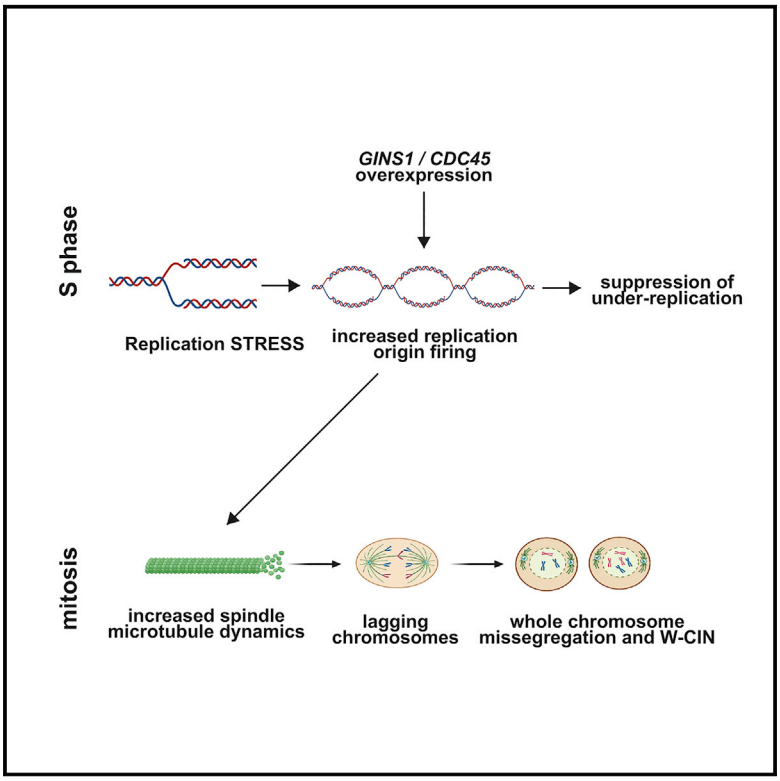


## Highlights

- Overexpression of origin firing genes correlates with W-CIN in cancer
- Increased origin firing is sufficient to trigger chromosome missegregation and CIN
- Mild replication stress results in increased origin firing and W-CIN
- Origin firing triggers increased microtubule dynamics in mitosis to trigger W-CIN

## Authors

Nicolas Böhly, Ann-Kathrin Schmidt, Xiaoxiao Zhang, Benjamin O. Slusarenko, Magdalena Hennecke, Maik Kschischo, Holger Bastians

## Correspondence

holger.bastians@uni-goettingen.de

## In brief

Chromosomal instability (CIN) is a hallmark of cancer. Böhly et al. show that increased replication origin firing, triggered by replication stress or overexpression of origin firing genes, causes increased microtubule dynamics in mitosis, which leads to whole-chromosome missegregation and CIN.

Böhly et al., 2022, Cell Reports *41*, 111836
December 13, 2022 © 2022 The Author(s).
https://doi.org/10.1016/j.celrep.2022.111836

CellPress

Cell Reports

CellPress
OPEN ACCESS

Article

# Increased replication origin firing links replication stress to whole chromosomal instability in human cancer

Nicolas Böhly,[1,4] Ann-Kathrin Schmidt,[1,4] Xiaoxiao Zhang,[2,3,4] Benjamin O. Slusarenko,[1] Magdalena Hennecke,[1] Maik Kschischo,[2] and Holger Bastians[1,5,*]

[1]Georg August University Göttingen, University Medical Center Göttingen (UMG), Department of Molecular Oncology, Section for Cellular Oncology, 37077 Göttingen, Germany

[2]University of Applied Sciences Koblenz, Department of Mathematics and Technology, 53424 Remagen, Germany

[3]Technical University of Munich, Department of Informatics, 81675 Munich, Germany

[4]These authors contributed equally

[5]Lead contact

*Correspondence: holger.bastians@uni-goettingen.de

https://doi.org/10.1016/j.celrep.2022.111836

## SUMMARY

Chromosomal instability (CIN) is a hallmark of cancer and comprises structural CIN (S-CIN) and numerical or whole chromosomal CIN (W-CIN). Recent work indicated that replication stress (RS), known to contribute to S-CIN, also affects mitotic chromosome segregation, possibly explaining the common co-existence of S-CIN and W-CIN in human cancer. Here, we show that RS-induced increased origin firing is sufficient to trigger W-CIN in human cancer cells. We discovered that overexpression of origin firing genes, including *GINS1* and *CDC45*, correlates with W-CIN in human cancer specimens and causes W-CIN in otherwise chromosomally stable human cells. Furthermore, modulation of the ATR-CDK1-RIF1 axis increases the number of firing origins and leads to W-CIN. Importantly, chromosome missegregation upon additional origin firing is mediated by increased mitotic microtubule growth rates, a mitotic defect prevalent in chromosomally unstable cancer cells. Thus, our study identifies increased replication origin firing as a cancer-relevant trigger for chromosomal instability.

## INTRODUCTION

Chromosomal instability (CIN) is a hallmark of human cancer and correlates with tumor progression, development of therapy resistance, and poor clinical outcome.[1–3] CIN can be categorized into two major forms: numerical or whole chromosomal instability (W-CIN), leading to aneuploidy, and structural CIN (S-CIN), which causes structural chromosomal aberrations, including deletions, insertions, and amplifications.[2] S-CIN can be mechanistically traced back to errors in DNA repair and to abnormal or slow DNA replication, a condition known as replication stress (RS).[4–6] On the other hand, W-CIN is caused by errors during chromosome segregation in mitosis. Various defects during mitosis have been suggested to contribute to W-CIN, including supernumerary centrosomes, spindle abnormalities, and impaired spindle checkpoint function.[1,7,8] It is well established that a major mitotic abnormality in chromosomally unstable cancer cells (W-CIN+ cells) is the appearance of lagging chromosomes during anaphase, which is the result of erroneous and hyperstable microtubule-kinetochore attachments leading to whole-chromosome missegregation.[9–11] It has been shown that an abnormal increase in microtubule growth rates in mitotic spindles can be a direct trigger for generation of lagging chromosomes and W-CIN.[10,12–15] Increased microtubule growth is a widespread mitotic defect in W-CIN+ cancer cells.[10,13,15] Correction of this defect in various CIN+ cancer cells is sufficient to suppress chromosome missegregation and W-CIN, indicating a causality between increased microtubule polymerization rates and induction of aneuploidy in cancer cells.[10,13,15] In cancer cells, aneuploidy is often accompanied by structural chromosome aberrations and vice versa, suggesting a link between W-CIN and S-CIN. Evidence of such a link was provided by demonstrating that W-CIN+ cells also suffer from RS. Rescuing RS in these cancer cells resulted in suppression of W-CIN, indicating that RS might link S-CIN to mitosis-mediated W-CIN.[16,17] Mechanistically, it has been demonstrated that moderate RS can cause premature centriole disengagement, which can contribute to spindle multipolarity in mitosis, supporting missegregation of mitotic chromosomes.[18] However, W-CIN+ cells only exhibit signs of very mild RS, which is associated with increased mitotic microtubule growth rates, leading to generation of lagging chromosomes as a cause of W-CIN.[17] Thus, there already is evidence of RS affecting mitotic chromosome segregation to cause W-CIN. However, the role of RS in induction of mitotic defects is unknown.

RS can be caused by various means, including DNA damage, abnormal DNA structure, and shortage of replication factors or nucleotides.[4,6] RS is prevalent in human cancer and


This is an open access article under the CC BY license (http://creativecommons.org/licenses/by/4.0/).

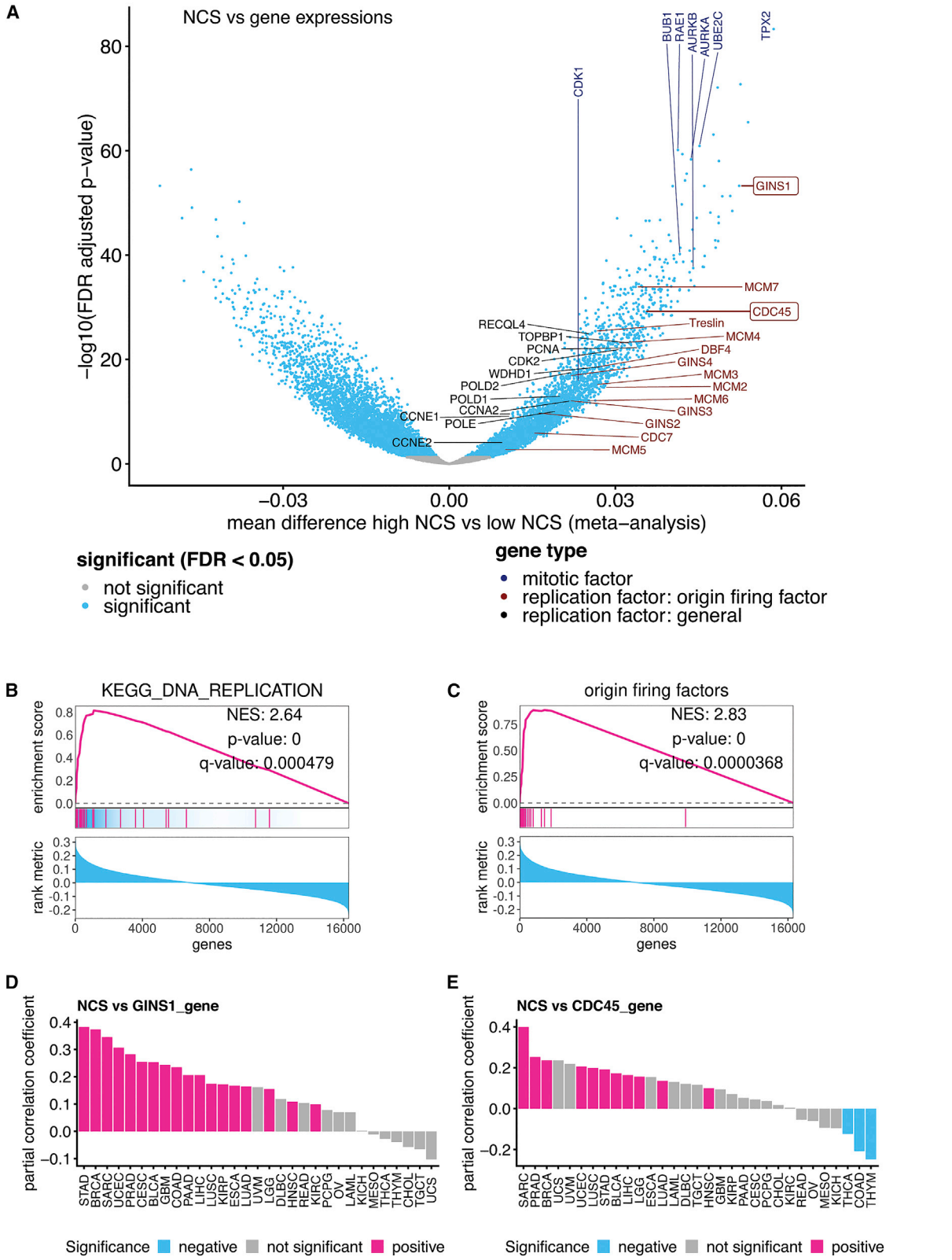


*(legend on next page)*

pre-cancerous lesions and has been associated with S-CIN. Oncogene activation, including *MYC* or *CCNE1* amplification, has been linked to induction of RS and genome instability.[19–22] Experimentally, inhibition of DNA polymerases using aphidicolin is widely used to induce RS, allowing induction of gradual levels of RS.[17] Cells respond to severe RS by activating a cell cycle checkpoint that involves the ATR and Chk1 kinases. The checkpoint function of ATR/Chk1 prevents S phase progression and entry into mitosis by inhibiting CDK activity while preventing progression of DNA replication by inhibiting late origin firing and stabilizing replication forks to allow subsequent re-start of replication during S phase.[23,24] The replication checkpoint is highly conserved and has been studied extensively in lower eukaryotes, most notably in budding yeast, where Mec1 (ATR) and Rad53 (Chk1) are activated in response to RS, inhibit late origin firing in S phase, and prevent premature entry into mitosis.[25,26] In yeast, Mec1 is also activated during an unperturbed cell cycle to monitor dNTP levels required for replication initiation[27] and prevent premature origin firing.[28]

In contrast to severe RS, which is associated with checkpoint activation and a profound effect on cell cycle progression, W-CIN+ cancer cells typically exhibit only very mild RS, which escapes the checkpoint control despite the presence of functional checkpoint components.[16,17] These cancer cells can enter mitosis, where under-replicated DNA might interfere with normal chromosome segregation.[29,30]

Initiation of DNA replication is highly conserved from yeast to man.[31,32] In preparation for DNA replication, human cells assemble ~500,000 pre-replication complexes (pre-RCs) in G1 phase by loading MCM helicase complexes (Mcm2–Mcm7) and additional licensing factors on specific chromatin sites, called origins of replication (ORIs), forming licensed origin recognition complexes (ORCs). At the onset of S phase, replication origin firing is triggered by Cdc7-Dbf4 and CDK kinases, which phosphorylate MCMs and promote recruitment of additional firing factors, including the GINS complex (Gins1–Gins4) and Cdc45 to form the active Cdc45-Mcm-Gins (CMG) helicase complex.[31–34] During an unperturbed S phase, only ~10%–30% of the licensed origins are fired, indicating that most licensed origins serve as backups. Upon RS, additional origins are activated, leading to a higher origin density on chromatin (i.e., associated with reduced inter-origin distances), and it is assumed that this represents a compensating mechanism to complete DNA replication before mitosis despite the presence of slowed replication.[35–38] However, the mechanisms leading to additional origin firing in mammals are not well understood, and it remains unclear whether additional origin firing during RS occurs at pre-defined sites or in a stochastic manner. In budding yeast, however, it is known that Mec1 and its downstream target Rad53 limit origin firing by directly targeting Sld3 (Treslin in mammals) and Dbf4/Cdc7, both of which are essential factors for further recruitment of origin firing factors, including Gins1 and Cdc45, to the firing replication fork.[39–41] In line with a key role of Mec1 in suppressing origin firing, *mec1-100* mutant cells, which only weakly activate Rad53, show excessive origin firing during S phase.[42,43] Similarly, in human cells, S phase-specific ATR inhibition is sufficient to induce additional origin firing, indicating that low ATR activity limits origin firing during an unperturbed S phase.[44–47] In this context, it has been proposed that ATR acts as a negative regulator of CDK1 during S phase by negatively controlling assembly of the Cdc7-counteracting RIF1-PP1 protein phosphatase complex.[48–50] Upon RS or ATR-RIF1 inhibition, additional origin firing is activated in a Cdc7-dependent manner, supporting completion of DNA replication even when forks progress slowly.[33,35] Thus, RS-induced origin firing seems to be beneficial for cells and is believed to suppress CIN.

In contrast to this view, we found in this study that genes directly involved in replication origin firing are positively correlated with W-CIN in human tumor samples, suggesting a role of increased origin firing in cancer CIN. We demonstrate that unscheduled induction of origin firing is sufficient to trigger W-CIN by increasing microtubule growth rates and chromosome missegregation in mitosis. We show that chromosomally unstable cancer cells not only suffer from mild RS but are also characterized by increased origin firing, leading to whole-chromosome missegregation and W-CIN in these cancer cells.

## RESULTS

### Genes involved in DNA replication origin firing are upregulated in human cancer and significantly correlated with W-CIN

To identify cancer-relevant genes that are associated with W-CIN in human cancer, we performed comprehensive pan-cancer analyses using data from 33 different cancer types from The Cancer Genome Atlas (TCGA) as detailed previously.[51] To quantify the degree of W-CIN in bulk tumor samples, we computed the numerical complexity score (NCS) using copy number segment data as a surrogate measure for W-CIN.[16,52]

**Figure 1. Positive association of genes involved in DNA replication origin firing with W-CIS in human cancer specimens**

(A) Association of gene expression and W-CIN in human cancer samples. The volcano plot shows the mean difference in normalized gene expression in tumor samples with high versus low NCS as a proxy measure for W-CIN. The NCS mean differences are adjusted for cancer type-specific effects in the 33 different tumor types included in the pan-cancer analysis, and the p values are adjusted for multiple testing.

(B) Gene set enrichment analysis for NCS and genes involved in DNA replication. The analysis was performed using a gene set annotated for DNA replication from the KEGG database. The significance for the normalized enrichment score (NES) was evaluated by a permutation test, and the pink bars indicate the position of DNA replication genes.

(C) Gene set enrichment analysis for NCS and genes associated with DNA replication origin firing. The analysis was performed using a set of manually curated origin firing factors. The significance for the NES was assessed by a permutation test, and the pink bars indicate the position of the origin firing genes.

(D) *GINS1* gene expression is positively correlated with NCS in multiple cancer types independent of the proliferation rates. The partial correlation coefficient accounts for the effect of proliferation rate estimates.

(E) *CDC45* gene expression is positively correlated with NCS scores in multiple cancer types independent of the proliferation rate.

See also Figures S1 and S2 and Table S1.

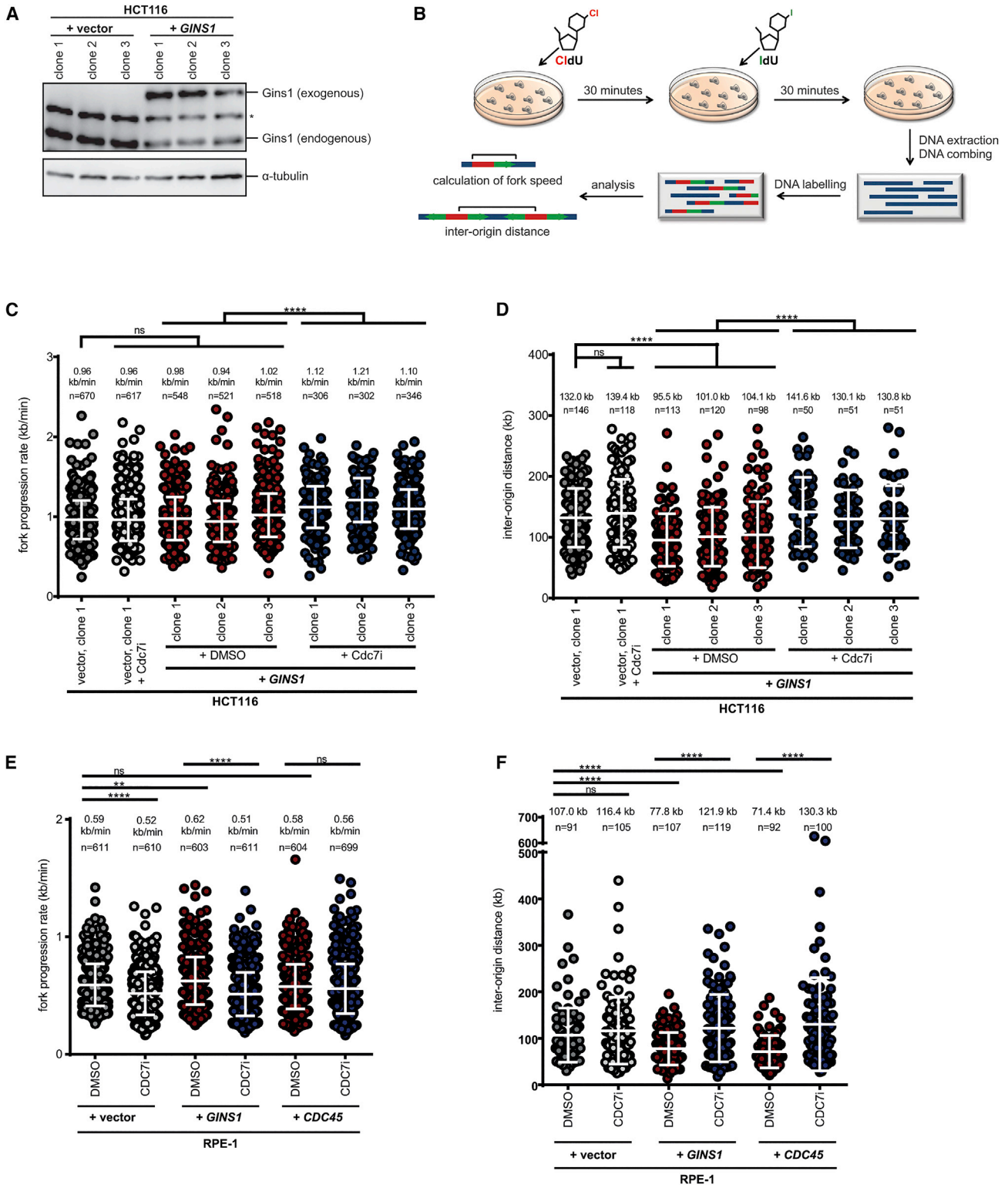


**Figure 2. *GINS1* overexpression increases replication origin firing without affecting replication fork progression**

(A) Generation of chromosomally stable HCT116 cells with stable *GINS1* overexpression. A representative western blot shows expression of endogenous and overexpressed Myc-FLAG-tagged *GINS1* (exogenous) in three independent HCT116-derived single cell clones. Single cell clones transfected with an empty vector served as a control. α-Tubulin was used as a loading control. An asterisk indicates an nonspecific protein band.

*(legend continued on next page)*

To filter genes differentially expressed in W-CIN tumors, we divided the tumor samples into high- and low-NCS groups and compared their mean gene expression corrected for cancer type-specific effects. Among the genes that positively correlate with the NCS across most cancer types, we found mitotic genes, including *TPX2*, *RAE1*, *UBE2C*, *AURKA*, *AURKB*, *BUB1*, and *CDK1* (Figure 1A). These genes, with known functions in mitotic chromosome segregation, are expected to be tightly associated with W-CIN and have been identified previously as part of a CIN gene signature,[53] validating our systematic and unbiased bioinformatics approach. Our analysis also identified upregulation of the known oncogenes *CCNE1* and *CCNE2* (encoding for cyclin E1/2) as being associated with high W-CIN. *CCNE1* amplification has been linked previously to RS and genome instability.[19–22] Our analysis revealed an overall strong association of W-CIN with high expression of genes involved in DNA replication, including *GINS1–GINS4*, *CDC45*, *MCMs*, *DBF4*, *CDC7*, *TRESLIN*, *RECQL4*, *PCNA*, *POLE*, and *POLD2* (Figure 1A). Gene set enrichment analysis showed that genes positively associated with NCS are highly enriched for DNA replication factors (permutation test $q < 0.0005$; Figure 1B) in comparison with other KEGG pathways (Table S1). A gene set annotated for DNA replication origin firing was found to be highly enriched at the top of all genes ranked by the association between their expression and NCS (permutation test $q < 0.0001$; Figure 1C), indicating that high expression of genes involved in replication origin firing is strongly associated with W-CIN. Our GSEA analysis is based on the rank of partial correlation coefficients between NCS and gene expression controlling the effect of proliferation rate, which is often considered a potential confounding variable of CIN.

To investigate the association between W-CIN and origin firing gene expression, such as *GINS*, *MCM*, and *CDC45*, in individual cancer types, we calculated Spearman correlation coefficients between gene expression and NCS. A strong correlation was reflected in many cancer types, as shown in Figure S1A. Among the top genes involved in origin firing whose expression correlate with W-CIN were *GINS1* and *CDC45* (Figure 1A and S1A), both of which are well known key regulators of replication origin firing.[33] *GINS1* and *CDC45* expression showed a strong positive correlation with high NCS in various tumor entities, even when predicted proliferation rates were taken into account,[54] suggesting that these origin firing genes might regulate W-CIN independent of overall proliferation in cancer specimens (Figures 1D and 1E). We also found that copy number variations (CNVs) of many origin firing factors show an overall strong positive correlation with NCS and are highly significant for *GINS1* (Figure S1B). These results suggest that amplification of origin firing genes is a frequent event in various human cancers and correlates with their high expressions and W-CIN. We also observed that overall CIN, measured by the weighted genome integrity index (WGII), and upregulation of origin firing genes, including *GINS1* and *CDC45*, are highly correlated (Figures S2A–S2C). This could be explained by the strong correlation between NCS and WGII (Pearson coefficient, 0.99; Figure S2D). Based on these results, we suggest that genes involved in origin firing, and in particular *GINS1* and *CDC45*, are potential oncogenes overexpressed in human cancer and might promote W-CIN.

### *GINS1* or *CDC45* overexpression increases replication origin firing without affecting replication fork progression

Our bioinformatics analysis identified the replication origin firing genes *GINS1* and *CDC45* as significantly associated with W-CIN. To analyze the effects of high *GINS1* and *CDC45* expression on a cellular level and on genome stability, we overexpressed *GINS1* or *CDC45* in chromosomally stable HCT116 cells, which are characterized by proper chromosome segregation and DNA replication.[10,17] Single cell clones stably expressing *GINS1* or *CDC45* were selected for further analysis (Figure 2A and S3A). *GINS1*- and *CDC45*-overexpressing cells showed no consistent alterations in the protein levels of other proteins involved in origin firing, including Mcm2, Mcm4, Mcm6, Cdc7, or Gins2 (Figure S3B). By performing cell cycle analysis and bromodeoxyuridine (BrdU) incorporation assays using synchronized cells with or without *GINS1*/*CDC45* overexpression, we found neither evidence of accelerated or delayed progression of S phase nor of altered mitotic entry (Figures S4A–S4E).

We then investigated in more detail how overexpression of the origin firing genes *GINS1* or *CDC45* affects DNA replication. For this, we performed DNA combing analysis upon DNA pulse labeling with the nucleoside analogs 5-chloro-2'-deoxyuridine (CldU) and 5-iodo-2'-deoxyuridine (IdU) (Figure 2B). Significantly, *GINS1* or *CDC45* overexpression did not affect the replication fork progression rate compared with parental HCT116 cells (Figures 2C and S5A). However, it significantly decreased the inter-origin distance, indicating the presence of increased numbers of firing origins upon *GINS1* or *CDC45* overexpression (Figures 2D and S5B). Thus, *GINS1*/*CDC45* overexpression is

(B) Scheme illustrating DNA combing to determine replication fork progression and inter-origin distances as a measure for origin firing activity. Cells are pulse labeled with 100 μM 5-chloro-2'-deoxyuridine (CldU) and 100 μM 5-iodo-2'-deoxyuridine (IdU) for 30 min each. DNA combing and subsequent detection of the newly synthesized DNA stretches allows calculation of DNA replication fork speed and inter-origin distance.
(C) Determination of replication fork progression rates in HCT116 cells with or without *GINS1* overexpression and additional CDC7 inhibition. The indicated single cell clones were pre-treated with 1 μM Cdc7 inhibitor (Cdc7i) XL-413 or DMSO as a control for 1 h before pulse label ing with nucleoside analogs. Scatter dot plots show values for fork progression rates (mean ± SD, t test).
(D) Determination of inter-origin distances as a measure for origin firing in HCT116 cells with or without *GINS1* overexpression and additional Cdc7 inhibition. Scatter dot plots show values for inter-origin distances (mean ± SD, t test).
(E) Determination of replication fork progression rates in RPE-1-hTert cells with or without *GINS1* or *CDC45* overexpression and additional Cdc7 inhibition. Transfected cells were pre-treated with 1 μM Cdc7i XL-413 or DMSO before pulse labeling with nucleoside analogs. Scatter dot plots show values for fork progression rates (mean ± SD, t test).
(F) Determination of inter-origin distances in RPE-1-hTert cells with or without *GINS1* or *CDC45* overexpression and additional Cdc7 inhibition. Scatter dot plots show values for inter-origin distances (mean ± SD, t test).
See also Figures S3–S5.

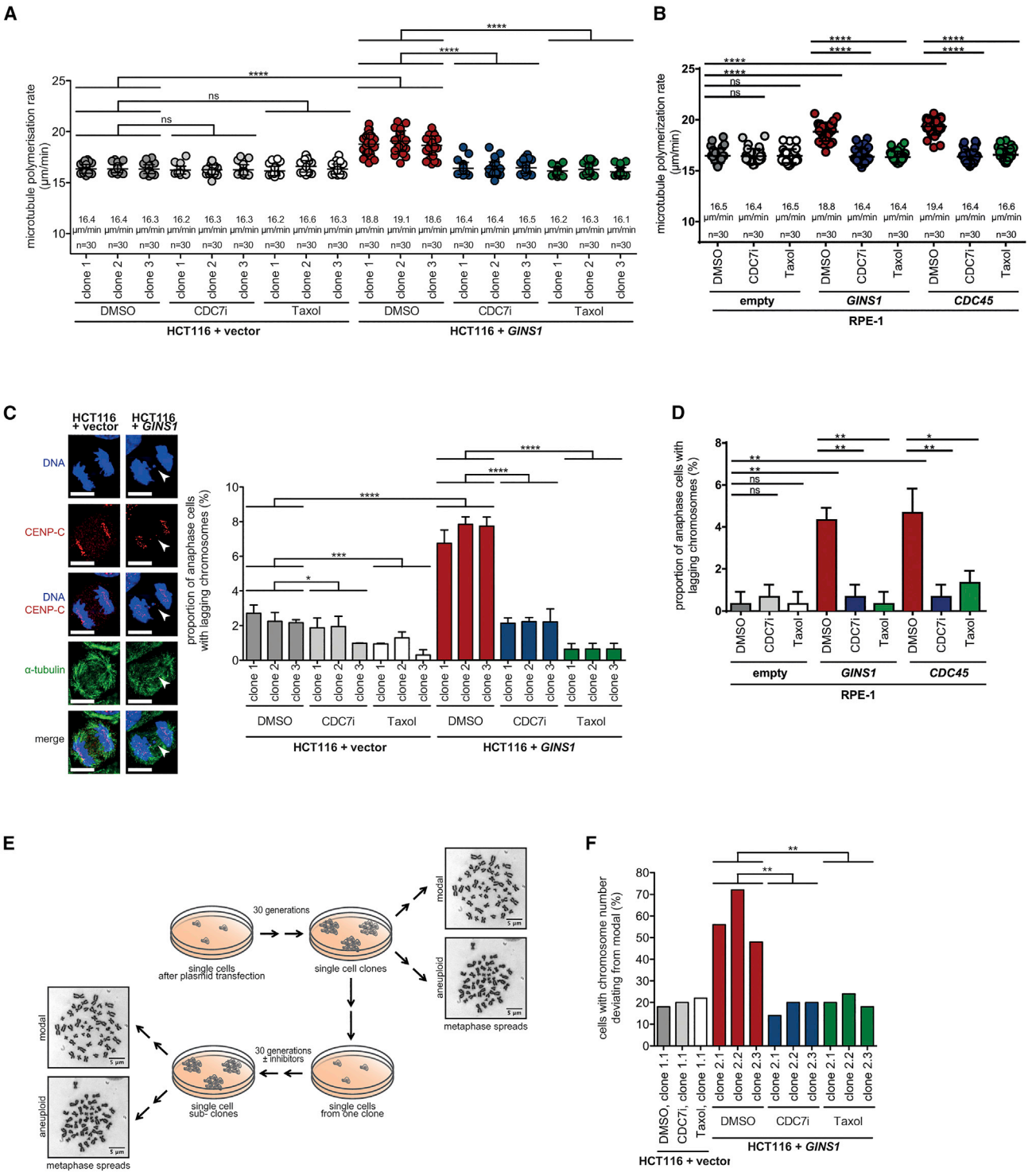


**Figure 3. Overexpression of *GINS1* or *CDC45* results in increased microtubule polymerization rates, chromosome missegregation, and W-CIN**

(A) Determination of mitotic microtubule growth rates in HCT116 cells with or without overexpression of *GINS1* and in the presence or absence of Cdc7 inhibition or low-dose Taxol treatment. The indicated single cell clones were treated with 1 µM of the Cdc7i XL-413, or with 0.2 nM Taxol for 16 h, and microtubule growth rates were determined in mitotic cells. Scatter dot plots show average microtubule growth rates (20 microtubules/cell, n = 30 mitotic cells, mean ± SD, t test).

*(legend continued on next page)*

sufficient to increase origin firing overall, but we cannot discriminate between firing of core and stochastic origins that are additionally activated (e.g., upon cell transformation), as demonstrated recently.[55]

In line with our findings that *GINS1/CDC45* overexpression causes increased origin firing but not slowed replication, we found neither evidence of the presence of under-replicated DNA in mitosis (as detected by FANCD2 foci on mitotic chromosomes; Figure S5C)[56] nor of induction of gross structural chromosome aberrations, including chromosome breaks or fusions (Figure S5D), in cells with increased origin firing.

Because origin firing at the beginning of S phase generally requires Cdc7-mediated phosphorylation,[32,33,57] we used the Cdc7 kinase inhibitor XL-413[58] to suppress origin firing. In fact, low concentrations of XL-413, which do not abrogate DNA replication, S phase progression, or proliferation, restored normal inter-origin distances and, thus, suppressed abnormally increased origin firing (Figure 2D). Cdc7 inhibition also slightly improved fork progression (Figure 2C), which might be due to increased availability of nucleotides when the number of firing origins is decreased upon Cdc7 inhibition, as suggested previously.[59] In addition to chromosomally stable HCT116 cells, we also overexpressed *GINS1* or *CDC45* in non-transformed diploid human retina pigment epithelial (RPE-1-hTert) cells (Figure S5E). DNA combing analysis revealed the same effects as seen for HCT116 cells; *GINS1/CDC45* overexpression resulted in an increase in the number of fired origins with only minor effects on replication fork progression. In RPE-1 cells, increased origin firing was efficiently and selectively suppressed upon partial Cdc7 inhibition (Figures 2E and 2F).

Our data indicate that *GINS1* or *CDC45* overexpression is a common event in human cancer and causes increased replication origin firing in chromosomally stable cells without affecting DNA replication and fork progression per se.

## Increased replication origin firing upon *GINS1* or *CDC45* expression causes increased microtubule dynamics in mitosis, leading to chromosome missegregation and W-CIN

Previous work showed that W-CIN+ cancer cells are characterized by perpetual chromosome missegregation. At the same time, they suffer from mild RS.[16,17] It has been demonstrated that chromosome missegregation and W-CIN in these cancer cells are triggered by abnormally increased microtubule growth rates during mitosis.[10,12,13,17] Therefore, we evaluated whether increased origin firing triggers increased microtubule growth rates and chromosome missegregation in mitosis. EB3-GFP tracking experiments in living mitotic cells revealed that overexpression of *GINS1* or *CDC45* in HCT116 or RPE-1 cells was sufficient to cause increased mitotic microtubule growth rates (Figures 3A, 3B and S6A) to a level typically detected in chromosomally unstable cancer cells.[10,13,17] Concomitantly, we detected a clear induction of lagging chromosomes during anaphase, indicative of whole-chromosome missegregation in HCT116 or RPE-1 cells with *GINS1* or *CDC45* overexpression (Figures 3C, 3D, and S6B). Chromosome missegregation was suppressed upon restoration of proper microtubule growth rates by low doses of Taxol (Figures 3A–3D, S6A, and S6B) or upon partial depletion of the microtubule plus-end polymerase chTOG/CKAP5[60](Figures S6C–S6E), which has been shown previously to correct abnormal microtubule growth rates in cancer cells.[10,13] Microtubule growth rates and lagging chromosomes were also suppressed by Cdc7 inhibition using XL-413 (Figures 3A–3D, S6A, and S6B), demonstrating that chromosome missegregation is not only dependent on increased microtubule growth rates but also on increased origin firing upon *GINS1* or *CDC45* overexpression. Finally, we tested whether *GINS1* or *CDC45* expression is sufficient to induce W-CIN. For this, we analyzed single cell clones with stable expression of *GINS1/CDC45* that were grown for 30 generations and determined the proportion of cells harboring chromosome numbers deviating from the modal number of 45 chromosomes (see scheme in Figure 3E). These karyotype analyses indicated that overexpression of *GINS1* or *CDC45* is sufficient to cause induction of aneuploidy and, thus, of W-CIN (Figures S6F and S6G). To investigate whether abnormally increased microtubule growth and increased origin firing are responsible for induction of W-CIN, we grew single cell clones with *GINS1* overexpression and additional long-term treatment with DMSO (control), low-dose Taxol (to restore proper microtubule growth rates), or XL-413 (to suppress additional origin firing; Figure S7A) and again determined the evolved karyotype variability (see scheme in Figure 3E). Restoration of proper microtubule growth rates upon Taxol treatment and Cdc7 inhibition fully suppressed evolution

(B) Determination of mitotic microtubule growth rates in RPE-1-hTert cells with or without overexpression of *GINS1* or *CDC45* and in the presence or absence of Cdc7 inhibition or low-dose Taxol treatment. The transfected cells were treated with 1 μM CDC7i or with 0.2 nM Taxol for 16 h, and microtubule growth rates were determined in mitotic cells. Scatter dot plots show average microtubule growth rates (20 microtubules/cell, n = 30 mitotic cells, mean ± SD, t test).

(C) Quantification of anaphase cells showing lagging chromosomes upon *GINS1* overexpression. The indicated cell clones were treated as in (A), and the proportion of anaphase cells with lagging chromosomes was determined. Representative images of anaphase cells with or without lagging chromosomes (white arrows) are shown (scale bars, 10 μm). The bar graph shows quantification of cells with lagging chromosomes (n ≥ 300 anaphase cells from three to five independent experiments, mean ± SD, t test).

(D) Quantification of anaphase cells showing lagging chromosomes upon *GINS1* or *CDC45* overexpression in RPE-1-hTert cells. The bar graph shows quantification of cells with lagging chromosomes with or without additional treatment with CDC7i or low-dose Taxol (n = 300 anaphase cells from three independent experiments, mean ± SD, t test).

(E) Scheme illustrating generation and analysis of single cell clones for karyotype analyses as a measure for W-CIN. Representative images of chromosome spreads with a normal and an aberrant karyotype are shown, and chromosomes were counted from single cells (scale bars, 5 μm).

(F) Induction and suppression of W-CIN in *GINS1*-overexpressing HCT116 cells after treatment with Taxol or Cdc7i. The indicated single cell clones were grown for 30 generations in the presence of DMSO, CDC7i, or Taxol. The chromosome numbers per cell were determined from metaphase spreads. The bar graph shows the proportion of cells with a karyotype deviating from the modal (45 chromosomes in HCT116 cells; n = 50 metaphase spreads, t test).

See also Figures S6 and S7.

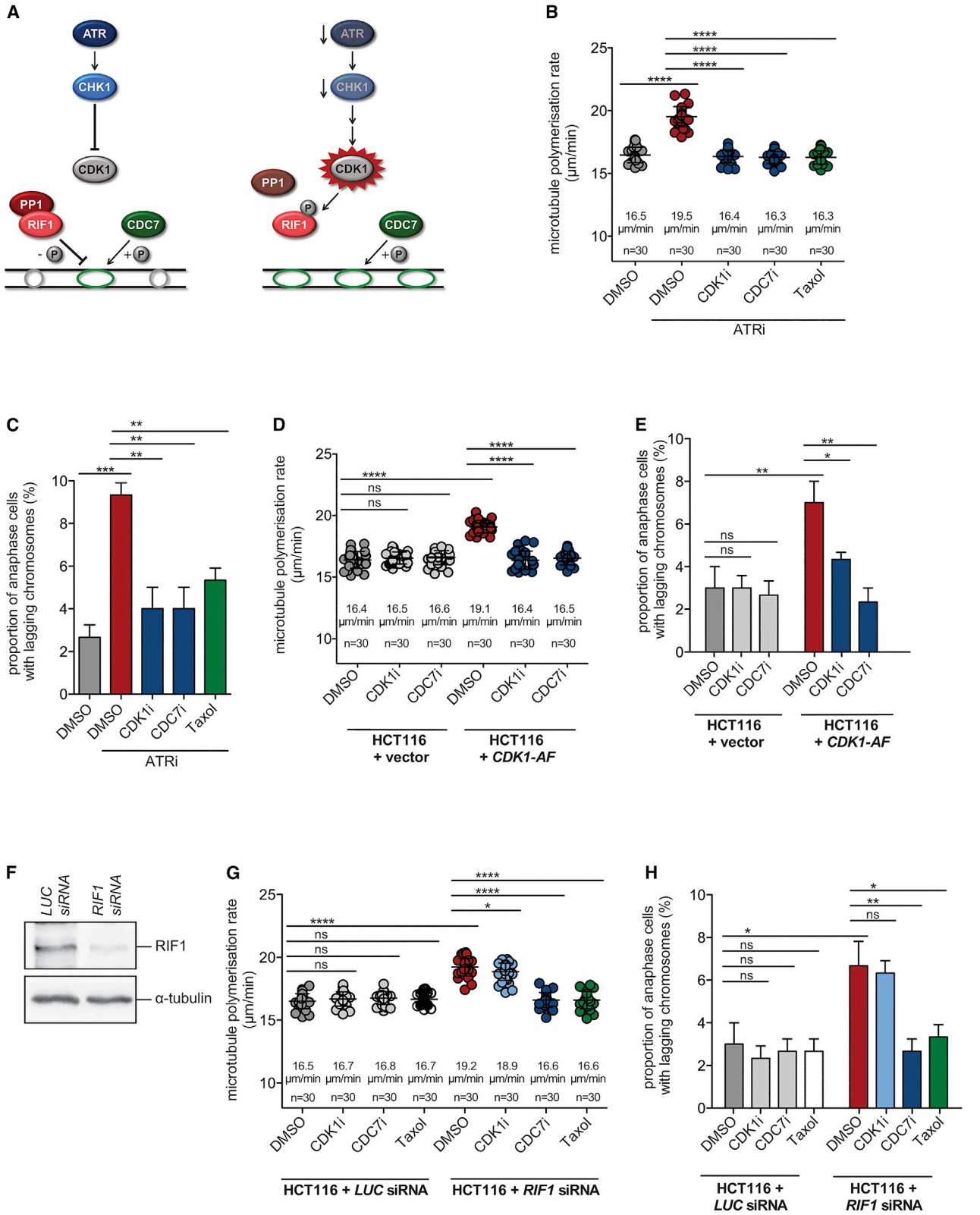


*(legend on next page)*

of aneuploidy, indicating that W-CIN, upon *GINS1* overexpression, is dependent on increased microtubule growth rates and increased origin firing (Figures 3F and S7B). We were not able to cultivate single cell clones in the continuous presence of 1.0 μM XL-413, which was used in transient experiments before; this might be due to intracellular accumulation of the inhibitor. Instead, we used 0.5 μM XL-413 in these long-term experiments, which was still sufficient to restore normal microtubule growth rates similar to 0.2 nM Taxol treatment (Figure S7C). These results demonstrate that increased origin firing induced by *GINS1 or CDC45* overexpression is sufficient to increase mitotic microtubule dynamics, triggering whole-chromosome missegregation and W-CIN, defects that are typically detected in W-CIN+ cancer cells.[10,13]

## ATR-CDK1-RIF1-regulated origin firing causes mitotic chromosome missegregation

Previous work from yeast and mammalian cells demonstrated a requirement for ATR (Mec1 in yeast) and Chk1 (Rad53) kinases to restrain origin firing in a Cdc7-dependent manner.[28,39–41] Recent work in human cells has shown that ATR signaling limits origin firing by counteracting CDK1 activity during S phase, allowing balanced action of Cdc7 and its counteracting RIF-PP1 phosphatase complex.[48,50] ATR inhibition has been shown to result in unleashed CDK1 activity that inactivates RIF1-PP1 and fosters increased origin firing in a Cdc7 kinase-dependent manner[48] (see scheme in Figure 4A). Based on these previous findings, we inhibited ATR and verified the increase in the number of firing origins in a CDK1- and Cdc7-dependent manner by performing DNA combing analyses (Figure S8A). These analyses also revealed a decrease in fork progression upon ATR inhibition that was rescued by Cdc7 but even further decreased after CDK1 inhibition (Figure S8B). Thus, ATR seems to regulate origin firing and fork progression, but, in line with the model, CDK1 downstream of ATR appears to positively regulate only origin firing.

We then investigated the mitotic outcome of ATR inhibition. ATR inhibition resulted in an increase in microtubule growth rates and chromosome missegregation in mitosis, both of which were suppressed upon inhibition of CDK1 or Cdc7, suggesting that ATR inhibitor-induced mitotic errors are mediated by origin firing rather than by reduced fork speeds (Figures 4B and 4C).

Because origin firing rather than fork progression after ATR inhibition is regulated by CDK1, we decided to directly increase CDK1 by stable expression of a constitutive active *CDK1* mutant (CDK1-AF)[13] and found that increased CDK1 was sufficient to increase microtubule growth rates and chromosome missegregation, again in a CDK1 and Cdc7 activity-dependent manner (Figures 4D and 4E). These results support the model where ATR inhibition acts through increased CDK1 activity to induce additional origin firing in human cells.

To substantiate this model, we depleted *RIF1* by small interfering RNAs (siRNAs) (Figure 4F) and performed DNA combing analyses. Depletion of *RIF1* did not affect fork progression but resulted in an increase in origin firing, which was fully rescued by Cdc7 but not by CDK1 inhibition (Figures S8C and S8D). Increased origin firing upon *RIF1* depletion led to an increase in mitotic microtubule dynamics and chromosome missegregation, both of which were fully suppressed only by Cdc7 inhibition and Taxol treatment but not by CDK1 inhibition (Figures 4G and 4H).

Our results strongly support the model where ATR restrains CDK1 to allow RIF1 to counteract Cdc7 to prevent excessive origin firing. As a consequence, abrogation of the ATR-RIF1-CDK1 axis causes mitotic errors and chromosome missegregation.

## Activation of additional origin firing during S phase triggers mitotic errors

To investigate whether the ATR-CDK1-dependent increased origin firing acts specifically during S phase to cause mitotic dysfunction, we used inhibitor treatments during different phases of the cell cycle prior to analysis of mitotic phenotypes. We established a treatment schedule based on synchronized cells and used the calculated time span from treatment until

**Figure 4. ATR-CDK1-RIF1-regulated increased origin firing causes mitotic chromosome missegregation**

(A) Schematic illustrating regulation of origin firing by ATR-CDK1-RIF1 signaling. In unperturbed cells, ATR signaling limits CDK1 activity, which allows balanced activity of the Cdc7 kinase and the phosphatase complex RIF1-PP1. Upon ATR inhibition, CDK1 activity increases and causes dissociation of the RIF1-PP1 complex, resulting in Cdc7-dependent origin firing (based on Moiseeva et al., 2019c).

(B) Determination of mitotic microtubule growth rates upon ATR inhibition-induced origin firing. HCT116 cells were treated with 1 μM ATR inhibitor (ATRi) ETP-46464 in combination with DMSO, 1 μM RO-3306 (CDK1 inhibitor [CDK1i]), 1 μM XL-413 (CDC7i), or 0.2 nM Taxol for 16 h. Scatter dot plots show average microtubule growth rates per cell (20 microtubules/cell, n = 30 mitotic cells, mean ± SD, t test).

(C) Quantification of anaphase cells with lagging chromosomes after ATR inhibition-induced origin firing. HCT116 cells were treated as in (B), and the bar graph shows the proportion of anaphase cells with lagging chromosomes (n = 300 anaphase cells, mean ± SD, t test).

(D) Measurements of mitotic microtubule growth rates in cells with or without expression of constitutive active CDK1. HCT116 cells stably expressing CDK1-AF were treated with CDK1i or CDC7i, and scatter dot plots show average mitotic microtubule growth rates (20 microtubules/cell, n = 30 mitotic cells, mean ± SD, t test).

(E) Quantification of anaphase cells with lagging chromosomes upon increased CDK1 activity and CDK1i or CDC7i treatment. Cells were treated as in (D), and the incidence of lagging chromosomes in anaphase cells was determined (n = 300 anaphase cells, mean ± SD, t test).

(F) siRNA-mediated downregulation of RIF1. HCT116 cells were transfected with siRNAs targeting *LUCIFERASE* (*LUC*) or *RIF1*. A representative western blot detecting RIF1 downregulation and α-tubulin levels as a loading control is shown.

(G) Measurements of mitotic microtubule growth rates in cells with or without downregulation of RIF1 and treatment with CDK1i, CDC7i, or Taxol. After siRNA transfection, cells were treated with CDK1i, CDC7i, or Taxol for 16 h, and microtubule growth rates were measured. Scatter dot plots show average microtubule growth rates per cell (20 microtubules/cell, n = 30 mitotic cells, mean ± SD, t test).

(H) Quantification of anaphase cells with lagging chromosomes after downregulation of RIF1 and treatment with CDK1i, CDC7i, or Taxol. Cells were treated as in (G), and bar graphs show the proportion of anaphase cells with lagging chromosomes (n = 300 anaphase cells, mean ± SD, t test).

See also Figure S8.

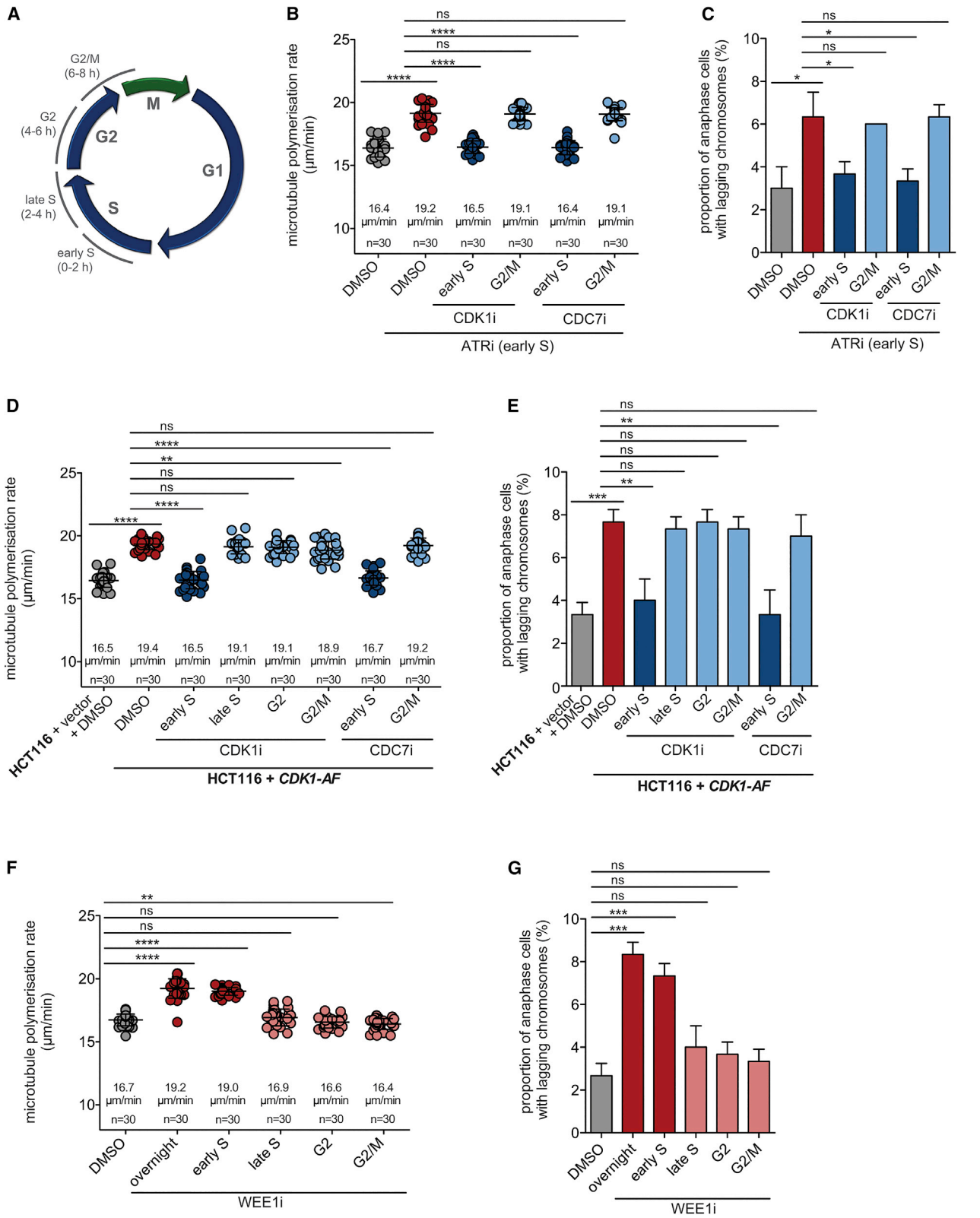


*(legend on next page)*

measurements in mitosis (Figure 5A). We treated cells with an ATR inhibitor only during a 2-h time window during early S phase, followed by washout of the drug. This S phase-specific treatment was sufficient to increase microtubule growth rates and induce lagging chromosomes in the subsequent mitosis (Figures 5B and 5C). The mitotic errors were only suppressed by CDK1 or Cdc7 inhibition when applied during early S phase but not when applied later, at G2/M transition (Figures 5B and 5C), indicating that the ATR inhibitor-mediated increase in CDK1- and Cdc7-mediated origin firing is required during S phase to induce errors in the subsequent mitosis. This finding was supported by using HCT116 cells with increased CDK1 activity (expressing CDK1-AF), where inhibition of CDK1 or Cdc7 only during early S phase, but not in late S phase, G2, or G2/M, rescued the mitotic defects (Figures 5D and 5E). Finally, we increased CDK1 activity in a cell cycle stage-dependent manner by inhibiting the Wee1 kinase, a well-known negative regulator of CDK1.[61] Wee1 inhibition has been shown previously to induce origin firing in a CDK1-dependent manner, which is in line with ATR functioning as a negative regulator of CDK1 in S phase (see scheme in Figure 4A).[49,62] Wee1 inhibition led to an increase in mitotic microtubule growth rates and to an induction of lagging chromosomes only when applied during a 2-h time window in early S phase, but not in late S phase, G2, or at G2/M (Figures 5F and 5G). Thus, increased origin firing, triggered upon mild RS or ATR inhibition or CDK1 activation in S phase, is sufficient to cause mitotic defects leading to whole-chromosome missegregation and W-CIN. However, the components targeted in our experiments, including ATR, RIF1, Wee1, CDK1, and Cdc7, have additional functions during S phase. Thus, we cannot exclude the possibility that induction of additional origin firing and induction of subsequent mitotic errors are a result of these additional functions.

## Additional origin firing induced by RS causes mitotic chromosome missegregation

Although severe RS can inhibit late origin firing in an ATR-dependent manner as part of a checkpoint response,[24] mild RS is known to activate additional origin firing, possibly reflecting a compensation mechanism to complete DNA replication when replication forks progress too slowly.[63] We wanted to determine whether additional origin firing induced by cancer-relevant mild RS can cause whole-chromosome missegregation in mitosis. We treated chromosomally stable HCT116 cells or non-transformed RPE-1 cells with 100 nM aphidicolin to induce mild RS during S phase and performed DNA combing analysis. As expected, low-dose aphidicolin reduced replication fork progression to a level typically seen in W-CIN + cancer cells[17](Figures 6A and 6B) and decreased the inter-origin distances, indicating that additional origin firing is associated with mild RS (Figures 6C and 6D). Importantly, Cdc7 (or CDK1) inhibition did not affect the slowed fork progression rates but fully restored normal inter-origin distances (Figures 6A–6D), indicating that partial Cdc7 inhibition suppresses increased origin firing during aphidicolin-induced mild RS. Then we tested whether increased origin firing induced by RS can trigger mitotic errors. As shown before,[17] mild RS increased mitotic microtubule growth rates and induced chromosome missegregation in mitotic HCT116 and RPE-1 cells (Figures 6E–6H). These effects were fully suppressed when origin firing was inhibited upon CDK1 or Cdc7 inhibition (Figures 6E–6H), which supports the notion that increased origin firing rather than slow fork progression during mild RS is a trigger for whole-chromosome missegregation during mitosis.

## Increased origin firing is a trigger for W-CIN in chromosomally unstable cancer cells

Chromosomally unstable, aneuploid colorectal cancer cells (W-CIN+ cells) are characterized by increased mitotic microtubule growth rates, increased incidence of lagging chromosomes, and mild RS.[10,13,16,17] We wanted to determine whether increased origin firing might link RS to W-CIN in these cancer cells. We performed DNA combing analysis using different W-CIN+ cell lines in the presence or absence of Cdc7 inhibition. In line with previous work,[16,17] we found that the W-CIN+ cells showed decreased replication fork progression rates compared with chromosomally stable HCT116 cells, and this was largely unaffected by Cdc7 inhibition (Figure 7A). All W-CIN+ cell lines showed increased firing of origins, reflected by decreased inter-origin distances, that was suppressed upon Cdc7 inhibition (Figure 7B), which is in full agreement with our results shown before. Abnormal microtubule growth rates and generation of lagging chromosomes were suppressed upon restoration of proper origin firing after Cdc7 inhibition (Figures 7C and 7D),

**Figure 5. Activation of additional origin firing during early S phase triggers mitotic errors**

(A) Depiction of cell cycle-dependent treatment windows. Cells were treated at specific time points during the cell cycle, and the effects were evaluated during the subsequent mitosis.

(B) Measurements of mitotic microtubule growth rates in HCT116 cells with S phase-specific ATR inhibition (1.0 μM ETP-46464) and additional CDK1i (1.0 μM RO-3306) or CDC7i (1.0 μM XL413) treatment during the indicated time windows. All drugs were washed out after 2 h of treatment, and microtubule growth rates were measured in mitosis. Scatter dot plots show average microtubule growth rates per cell (20 microtubules/cell, n = 30 mitotic cells, mean ± SD, t test).

(C) Quantification of anaphase cells with lagging chromosomes after cell cycle-specific drug treatments as used in (B). The proportion of anaphase cells with lagging chromosomes was determined (n = 300 anaphase cells, mean ± SD, t test).

(D) Measurements of mitotic microtubule growth rates in cells with elevated CDK1 activity (CDK1-AF) and treatment with CDK1i or CDC7i during the indicated time windows. Scatter dot plots show average microtubule growth rates per cell (20 microtubules/cell, n = 30 mitotic cells, mean ± SD, t test).

(E) Quantification of anaphase cells with lagging chromosomes using CDK1-AF-expressing cells with or without cell cycle-specific CDK1i and CDC7i treatment as used in (D). The proportion of anaphase cells with lagging chromosomes was determined (n = 300 anaphase cells, mean ± SD, t test).

(F) Measurements of mitotic microtubule growth rates in cells treated with 75 nM of the Wee1 inhibitor MK-1775 (WEE1i) for 2 h during the indicated cell cycle phases. Scatter dot plots show average microtubule growth rates per cell (20 microtubules/cell, n = 30 mitotic cells, mean ± SD, t test).

(G) Quantification of anaphase cells with lagging chromosomes after cell cycle-specific WEE1i treatment as used in (F). The proportion of anaphase cells with lagging chromosomes was determined (n = 300 anaphase cells, mean ± SD, t test).

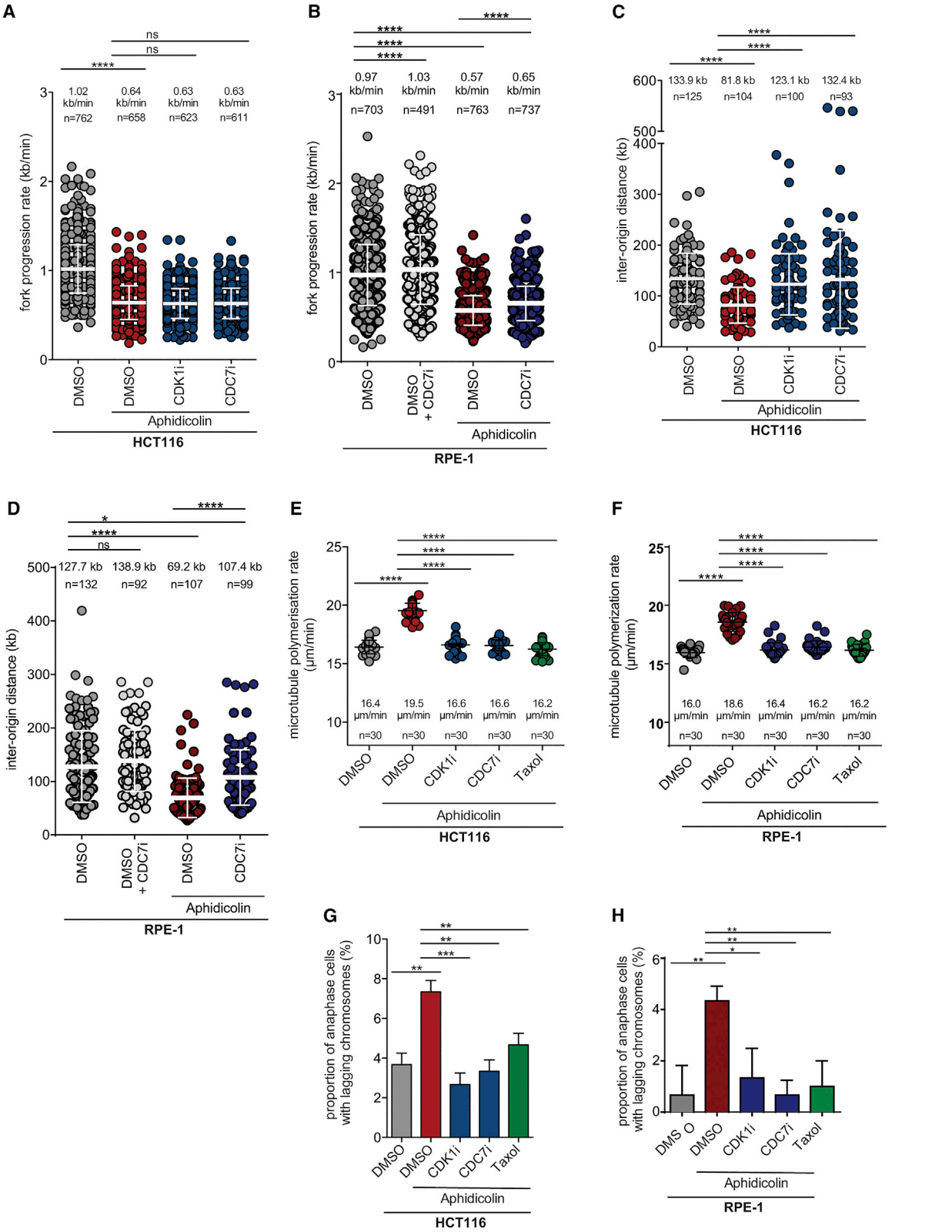


*(legend on next page)*

indicating that increased origin firing, but not slowed replication fork progression, acts as a trigger for subsequent mitotic errors. We showed recently that perpetual chromosome missegregation in W-CIN+ cells is suppressed upon CDK1 inhibition,[13] which is in line with our results presented here, showing that unleashed CDK1 activity upon ATR inhibition increases origin firing (Figure 4). To support our findings, we partially depleted Cdc7 or other components of the CMG helicase (Gins1, Cdc45, and Mcm2; Figures S9A–S9E), all of which are well known to influence origin initiation,[38,64] and analyzed microtubule growth rates and chromosome segregation in mitosis. Similar to Cdc7 or CDK1 inhibition, siRNA-mediated partial knockdown of *CDC7*, *GINS1*, *CDC45*, or *MCM2* restored normal mitotic microtubule polymerization rates and chromosome segregation in all three W-CIN+ cell lines (Figures 7E, 7F, and S9F). Thus, increased origin firing seen in chromosomally unstable cancer cells suffering from mild RS acts as a trigger for subsequent mitotic chromosome missegregation and CIN.

## DISCUSSION

This study revealed that abnormally increased replication origin firing during S phase of the cell cycle can act as a so far unrecognized trigger for chromosome missegregation in the subsequent mitosis, constituting W-CIN in human cancer cells. We showed that induction of additional origin firing can occur in different scenarios: (1) upon overexpression of potentially oncogenic origin firing genes, causing increased origin firing associated with W-CIN in human cancer specimens; (2) upon inhibition of the ATR-RIF1 axis, known to negatively regulate origin firing in human cells during an unperturbed S phase;[35,48] (3) upon experimental induction of mild RS (RS) using the DNA polymerase inhibitor aphidicolin;[35,63] and (4) in W-CIN+ cancer cells known to exhibit endogenous mild RS.[16,17] In all cases, we found that additional origin firing, but not slowed replication, is sufficient to induce mitotic chromosome missegregation, W-CIN, and, thus, genome instability.

A key finding of our work is that the origin firing genes *GINS1* and *CDC45* are consistently upregulated and strongly correlated with W-CIN in many cancer types. In contrast to previous studies, where mainly upregulation of mitotic genes was found to be associated with W-CIN,[53] we found that high expression of *GINS1* and *CDC45* is associated with W-CIN and overall CIN independent of tumor proliferation. Genes annotated for "DNA replication" are even more strongly correlated with W-CIN than "cell cycle" genes, suggesting that alterations specifically in DNA replication have a highly significant effect on W-CIN, which is thought to be driven by mitotic errors. We also provide evidence of copy number gains as a source for overexpression of origin firing factors, including *GINS1*. This is also seen for mitotic genes such as *AURKA* and *TPX2*, also previously identified as being strongly associated with CIN. These genes are located on chromosome 20, which is known to be frequently gained in various human cancers.[53,65] We found that overexpression of the origin firing genes *GINS1* or *CDC45* alone is sufficient to trigger additional origin firing without inducing RS per se; i.e., without altering replication fork velocity. This indicates that overexpression of single origin firing genes in cancer can be sufficient to trigger activation of additional origins. The exact mechanism behind this remains to be determined. Specific induction of additional origin firing was sufficient to cause mitotic chromosome missegregation, aneuploidy, and W-CIN. Because W-CIN has been linked to tumor progression, tumor aggressiveness, and therapy resistance,[1,2] it is not surprising that high expression of *GINS1* or *CDC45* in cancer has been found to be associated with poor prognosis in different tumor types, supporting putative oncogenic functions of genes involved in origin firing.[66,67]

Other well-known oncogenes, such as *MYC* or *CCNE1*, have also been implicated in induction of abnormal origin firing. Expression of these oncogenes results in premature entry into S phase associated with induction of additional intragenic origins.[22] Whether this also causes mitotic errors and W-CIN has not been investigated in the context of origin firing, but previous studies have associated *MYC* and *CCNE1* expression with mitotic defects.[19,21,68,69]

In response to *GINS1/CDC45* overexpression and upon mild RS induction, we clearly detected additional origins to be activated, but we did not define the sites of origins. The nature

**Figure 6. RS-induced additional origin firing causes mitotic chromosome missegregation**

(A) Measurements of replication fork progression rates in chromosomally stable HCT116 cells upon mild RS and treatment with CDK1i or Cdc7i. Cells were treated with 100 nM aphidicolin to induce mild RS and additionally with DMSO, 1 μM RO-3306 (CDK1i), or 1 μM XL-413 (CDC7i) for 1 h. Subsequently, cells were subjected to DNA combing analysis, and replication fork progression rates were determined (mean ± SD, t test).

(B) Measurements of replication fork progression rates in RPE-1-hTert cells upon treatment with 100 nM aphidicolin and CDC7i. Cells were subjected to DNA combing analysis, and replication fork progression rates were determined (mean ± SD, t test).

(C) Measurements of inter-origin distances as a measure for origin firing frequencies. HCT116 cells were treated as in (A), and inter-origin distances were determined (mean ± SD, t test).

(D) Measurements of inter-origin distances in RPE-1-hTert cells after mild RS. Cells were treated as in (B), and inter-origin distances were determined (mean ± SD, t test).

(E) Determination of mitotic microtubule growth rates upon aphidicolin-induced mild RS and treatment with CDK1i or CDC7i. HCT116 cells were treated with 100 nM aphidicolin and CDK1i, CDC7i, or 0.2 nM Taxol for 16 h, and microtubule growth rates were measured in living mitotic cells. Scatter dot plots show average microtubule growth rates per cell (20 microtubules/cell, n = 30 mitotic cells, mean ± SD, t test).

(F) Determination of mitotic microtubule growth rates in RPE-1-hTert cells upon mild RS and treatment with CDK1i or CDC7i. Cells were treated with 100 nM aphidicolin and CDK1i, CDC7i, or 0.2 nM Taxol for 16 h, and microtubule growth rates were measured in living mitotic cells. Scatter dot plots show average microtubule growth rates per cell (20 microtubules/cell, n = 30 mitotic cells, mean ± SD, t test).

(G) Quantification of anaphase cells showing lagging chromosomes after induction of mild RS and treatment with CDK1i, CDC7i or Taxol. HCT116 cells were treated as in (A), and the bar graph shows the proportion of cells with lagging chromosomes (n = 300 anaphase cells, mean ± SD, t test).

(H) Quantification of RPE-1-hTert cells showing lagging chromosomes after induction of mild RS and treatment with CDK1i, CDC7i, or Taxol. Cells were treated as in (B), and the bar graph shows the proportion of cells with lagging chromosomes (n = 300 anaphase cells, mean ± SD, t test).

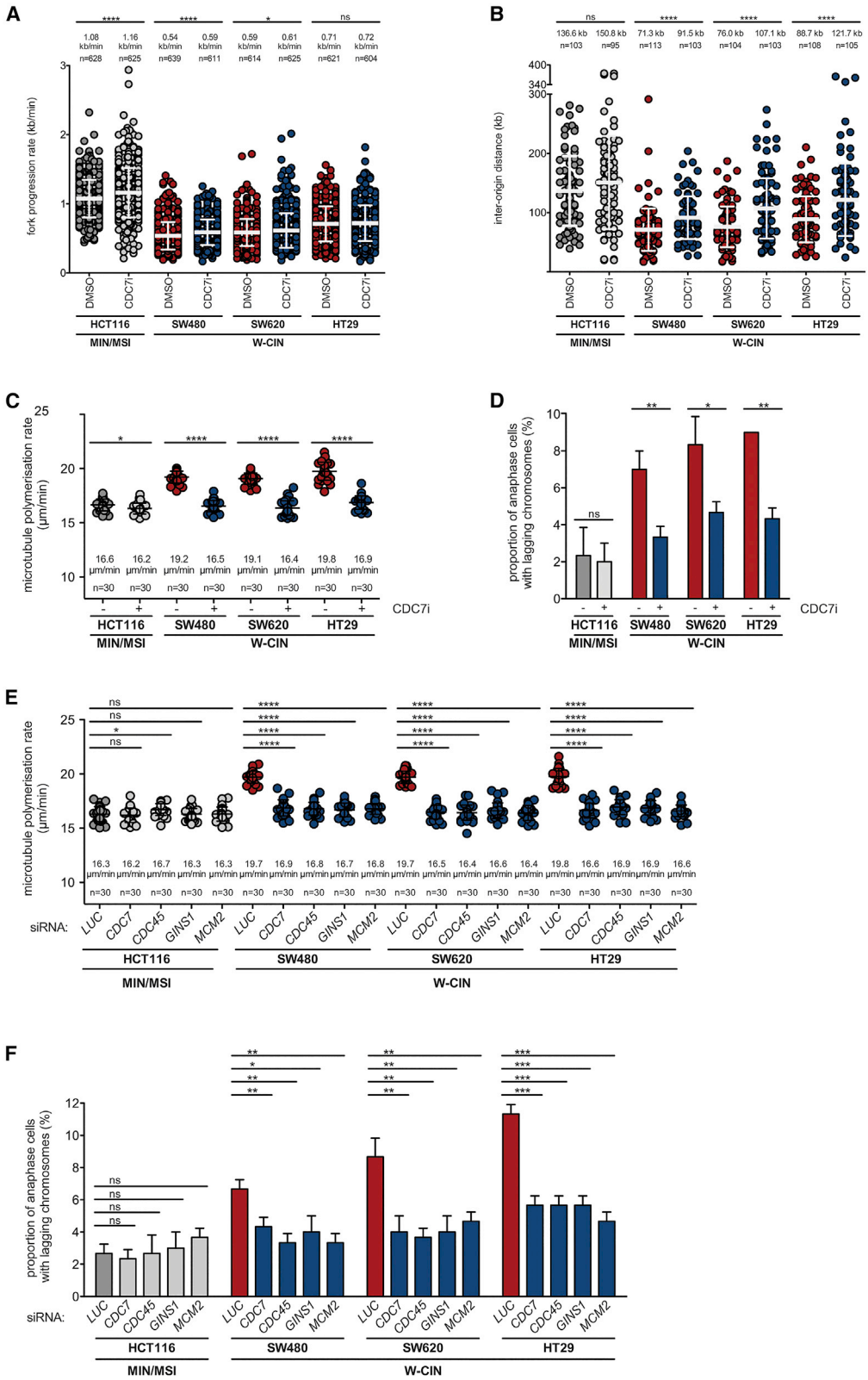


*(legend on next page)*

and structural characteristics of origins are not well understood, and it is unknown whether specific pre-defined origins are activated in response to RS. A recent study has demonstrated that unperturbed replication in normal cells is initiated mostly (80%) at so-called core origins, which are highly active, often associated with transcription, and defined by G-rich DNA motifs. Immortalized human cells, however, activate additional, stochastic origins that are preferentially associated with heterochromatin.[55] Whether RS or oncogene expression induces additional core or, rather, stochastic origins remains to be determined. In this context, it is interesting that our cell cycle-dependent analysis of origin firing induction revealed that there is a time window for origin firing during early S phase, which seems to be of particular importance for induction of W-CIN. It is well known that DNA replication has complex and distinct spatiotemporal organization and timing.[70] Late-replicating domains often show low origin densities, which might contribute to their under-replication in response to RS. These regions have been identified as common fragile sites (CFSs), which are prone to fragility and represent common breakpoints in cancer cells.[70,71] In contrast, early-replicating fragile sites (ERFS) are located in early-replicating chromosome domains and contain highly expressed genes and a higher origin density.[72] Whether ERFSs are generally associated with core origins is not known. Our results suggest that mitotic errors are more likely to result from increased origin firing in early S phase; i.e., possibly in early-replicating domains associated with high transcriptional activity. Thus, it is tempting to speculate that transcription-replication conflicts, which might be more prevalent upon increased origin firing in early-replicating domains,[73] might be involved in induction of mitotic errors. This point clearly deserves more detailed future investigations.

Based on previous studies, it is assumed that additional origin firing in response to RS is a rescue mechanism to minimize under-replication upon RS.[35,63] It is well known that origins are licensed in a 4- to 5-fold excess in G1 phase by assembling pre-RCs on origins,[31,32,64] and only a fraction of these licensed origins is activated at the beginning of S phase. Thus, there are large numbers of licensed origins that can act as backups, and some of them are activated under conditions of RS.[35,63] A causal link between RS and increased origin firing is supported by the observation that partial depletion of MCM2-7 complexes, which only impairs additional origin firing during RS, but not normal DNA replication timing, results in induction of markers for under-replicated DNA, including DNA damage, mitotic DNA synthesis, and formation of 53BP1 nuclear bodies.[36,38] Hence, RS-induced additional origin firing appears to be beneficial for cells and allows completion of replication even when replication fork progression is slowed.[35] Our DNA combing results support this view and show that aphidicolin-induced RS activates additional origins, similar to the situation seen upon *GINS1/CDC45* overexpression. However, in contrast to the general assumption, our results clearly indicate that additional origin firing is not beneficial per se but rather associated with induction of W-CIN and genome instability by directly affecting mitotic chromosome segregation. Thus, increased origin firing appears to be a double-edged sword and helps to rescue RS but also induces mitotic errors and CIN.

It is still unknown how RS triggers activation of additional origins in S phase. It has been suggested that licensed but dormant origins are passively removed during unperturbed DNA replication. Consequently, a subset of licensed origins might not be removed during RS because of the slowly progressing forks and are then allowed to fire.[35,63] In addition to this passive mechanism, active signaling might also be involved in triggering origin firing upon RS. It is well established that, in response to severe RS, the ATR-Chk1 (Mec1-Rad53 in yeast) checkpoint is activated and prevents late origin firing and further progression of S phase by targeting CDK or, in yeast, various origin firing factors.[23–26] However, CIN+ cancer cells typically suffer only from very mild RS, and this low level of RS does not activate the ATR-Chk1 checkpoint and allows progression of S phase and long-term proliferation.[17] It is interesting that, in addition to the checkpoint function of ATR, the same kinase also restrains origin firing during an unperturbed S phase. In human cells, ATR restrains CDK1 activity to counteract Cdc7 activity through RIF1 phosphorylation (see model in Figure 4A).[48] In line with this, we showed that inhibition of ATR or RIF1 or activation of CDK1 is sufficient to trigger additional origin firing and, subsequently, also mitotic errors in the absence of RS. However, because these key regulators might also have additional functions during S phase, we cannot exclude that, e.g., inhibition of ATR-RIF1 might affect origin firing in an indirect manner. Our results support the view that origin firing is under control of the

**Figure 7. Increased origin firing is a trigger for W-CIN in chromosomally unstable colorectal cancer cells**

(A) Measurements of replication fork progression rates in different W-CIN+ colorectal cancer cell lines in the presence or absence of CDC7i. The indicated cell lines were treated with CDC7i for 2 h and subjected to DNA combing analysis, and replication fork progression rates were determined (mean ± SD, t test).

(B) Measurements of inter-origin distances as a measure for origin firing frequencies. The different cell lines were treated as in (A), and inter-origin distances were determined (mean ± SD, t test).

(C) Measurements of mitotic microtubule growth rates in different CIN+ cells treated with CDC7i. The indicated colorectal cancer cell lines were treated with CDC7i for 16 h, and microtubule growth rates were determined in mitotic cells. Scatter dot plots show average microtubule growth rates per cell (20 microtubules/cell, n = 30 mitotic cells, mean ± SD, t test).

(D) Proportion of W-CIN+ cells with lagging chromosomes after CDC7i treatment. The indicated cell lines were treated as in (C), and the proportion of anaphase cells with lagging chromosomes was determined (n = 300 anaphase cells, mean ± SD, t test).

(E) Measurements of mitotic microtubule growth rates in W-CIN+ cells after downregulation of CDC7 or CMG components. The indicated cancer cell lines were transfected with siRNAs targeting *CDC7*, *CDC45*, *GINS1*, or *MCM2*. *LUC* siRNA was used a control. 48 h after transfection, microtubule growth rates were determined in mitotic cells. Scatter dot plots show average microtubule growth rates per cell (20 microtubules/cell, n = 30 mitotic cells, mean ± SD, t test).

(F) Proportion of W-CIN+ cells with lagging chromosomes after downregulation of CMG components. The indicated cell lines were transfected as in (E), and the proportion of anaphase cells with lagging chromosomes was determined (n = 300 anaphase cells, mean ± SD, t test).

See also Figure S9.

ATR-CDK1-RIF1 axis, and this might provide a possible link to the subsequent mitotic regulation because ATR, CDK1, and RIF1 also function in mitosis to regulate spindle assembly, anaphase bridge resolution, and chromosome segregation.[74,75]

It is intriguing that increased origin firing in S phase triggers chromosome missegregation in the subsequent mitosis. Our work presented here establishes a causal link between origin firing and an increase in microtubule dynamics in mitosis. Abnormally increased microtubule growth has been shown to induce whole-chromosome missegregation by affecting the positioning of the mitotic spindle, which facilitates formation of erroneous (merotelic) microtubule-kinetochore attachments that lead to generation of lagging chromosomes and missegregation in anaphase.[9,10] Erroneous kinetochore attachments, lagging chromosomes, and increased microtubule dynamics in mitosis are frequent mitotic defects in aneuploid cancer cells.[10,15,17,76] We now report another causative relationship between abnormal microtubule dynamics, mild RS, and increased origin firing and propose that additional origin firing is a driving force for microtubule dynamics-mediated induction of W-CIN in human cancer cells. How increased origin firing is mechanistically linked to regulation of microtubule dynamics is not yet understood and will be the subject of future studies. It is clear, however, that a number of proteins localized to the plus tips of microtubules act in concert to regulate microtubule growth rates.[77] One of these key proteins is ch-TOG/CKAP5, a processive microtubule polymerase that mediates incorporation of $\alpha/\beta$-tubulin dimers into the growing microtubule plus tip.[60] Ch-TOG is frequently upregulated in cancer cells,[78,79] and this is sufficient to increase mitotic microtubule growth rates (unpublished data). Here we show that partial repression of ch-TOG is sufficient to restore normal microtubule growth and suppresses chromosome missegregation in cells with *GINS1*/*CDC45* overexpression; i.e., in cells where microtubule growth is induced by increased origin firing (Fig. S6). This makes ch-TOG an attractive candidate to be regulated in response to abnormal origin firing. It is documented that ch-TOG is phosphorylated at many sites in cancer cells (www.phosphonet.ca), and several sites fit with consensus sites for ATR/ataxia telangiectasia mutated (ATM)-mediated phosphorylation (SQ sites), which might provide a possible link to S phase-related signaling, which will be an important subject of our future work.

### Limitations of study

We used various conditions that lead to increased origin firing, including mild RS, endogenous RS in CIN+ cancer cells, overexpression of *GINS1* or *CDC45*, and inhibition of ATR-RIF1. We used various conditions that lead to increased origin firing, including mild RS induced by lDNA pollymerase inhibition, endogenous RS in CIN+ cancer cells, overexpression of *GINS1* or *CDC45*, and inhibition of ATR-RIF1. Thus, it remains unknown whether the different conditions trigger the same or a different spectrum of origins in the genome. This question might be relevant for future studies investigating possible structural chromosome aberrations in response to additional origin firing. It would be interesting to determine whether certain positions of additional fired origins are associated with break points or with other chromosomal aberrations in cancer cells. In this regard, our study only provides a first glimpse. We found that induced origin firing does not cause gross chromosomal damage, which could be seen on chromosome spreads. We did not analyze possible induction of small and possibly recurrent chromosomal aberrations that might arise specifically upon increased origin firing. More detailed analyses of this are required, also to detect genomic aberrations in cancer samples characterized by overexpression of *GINS1*, *CDC45*, or other origin firing genes. Finally, although our study provides clear evidence of a role of additional origin firing in inducing whole-chromosome missegregation in the subsequent mitosis, it remains unknown at this point how origin firing is linked to the detected mitotic defects, most notably increased microtubule growth rates. Our previous work has provided first evidence showing that increased mitotic microtubule growth rates are associated with transient mispositioning of the mitotic spindle,[10] which might contribute to generation of erroneous merotelic microtubule-kinetochore attachments, as shown previously.[80] However, it is currently not clear how microtubule dynamics controls mitotic spindle positioning or how RS and increased origin firing are related to regulation of microtubule plus-end regulation. It seems plausible that additional origin firing could activate stress-related signaling pathways that target microtubule plus-end regulatory proteins in an unscheduled manner, finally leading to a specific increase in microtubule growth rates.

## STAR★METHODS

Detailed methods are provided in the online version of this paper and include the following:

- KEY RESOURCES TABLE
- RESOURCE AVAILABILITY
  - Lead contact
  - Materials availability
  - Data and code availability
- EXPERIMENTAL MODEL AND SUBJECT DETAILS
  - Mammalian cell lies and growth conditions
  - Generation of stable cell lines
- METHOD DETAILS
  - Plasmid and siRNA transfections
  - Cell treatments
  - Analysis of microtubule polymerization rates
  - Quantification of anaphase cells exhibiting lagging chromosomes
  - Detection of FANCD2 foci
  - Detection of W-CIN and gross structural aberrations
  - DNA combing assays
  - Western blotting
  - Flow cytometry analyses
  - TCGA molecular and ploidy data
  - Quantifying W-CIN
  - Quantifying overall CIN
  - Chromosome instability and gene expression association analysis
  - Correcting the confounding effect of proliferation rates
  - Chromosome instability and copy number association analysis
  - Gene set enrichment analysis
- QUANTIFICATION AND STATISTICAL ANALYSIS

## SUPPLEMENTAL INFORMATION

Supplemental information can be found online at https://doi.org/10.1016/j.celrep.2022.111836.

## ACKNOWLEDGMENTS

This work was supported by the Deutsche Forschungsgemeinschaft (FOR2800 for H.B. and M.K. and BA1698/12-1 for H.B.). We thank Helmut Pospiech, Linda Wordeman, Makoto Iimori, and Lienhard Schmitz for providing plasmids and Dominik Boos for help with BrdU FACS analyses.

## AUTHOR CONTRIBUTIONS

N.B., A.-K.S., X.Z., B.O.S., and M.H. designed and performed experiments and analyzed data. M.K. and H.B. designed the study and analyzed data. H.B. supervised the study and wrote the manuscript. All authors contributed to the manuscript.

## DECLARATION OF INTERESTS

The authors declare no competing interests.

Received: October 28, 2021
Revised: September 12, 2022
Accepted: November 22, 2022
Published: December 13, 2022

## REFERENCES

1. Ben-David, U., and Amon, A. (2020). Context is everything: aneuploidy in cancer. Nat. Rev. Genet. *21*, 44–62. https://doi.org/10.1038/s41576-019-0171-x.
2. Sansregret, L., Vanhaesebroeck, B., and Swanton, C. (2018). Determinants and clinical implications of chromosomal instability in cancer. Nat. Rev. Clin. Oncol. *15*, 139–150.
3. Lukow, D.A., Sausville, E.L., Suri, P., Chunduri, N.K., Wieland, A., Leu, J., Smith, J.C., Girish, V., Kumar, A.A., Kendall, J., et al. (2021). Chromosomal instability accelerates the evolution of resistance to anti-cancer therapies. Dev. Cell *56*, 2427–2439.e4. https://doi.org/10.1016/j.devcel.2021.07.009.
4. Wilhelm, T., Said, M., and Naim, V. (2020). DNA replication stress and chromosomal instability: dangerous liaisons. Genes *11*, 642. https://doi.org/10.3390/genes11060642.
5. Siri, S.O., Martino, J., and Gottifredi, V. (2021). Structural chromosome instability: types, origins, consequences, and therapeutic opportunities. Cancers *13*, 3056. https://doi.org/10.3390/cancers13123056.
6. Zeman, M.K., and Cimprich, K.A. (2014). Causes and consequences of replication stress. Nat. Cell Biol. *16*, 2–9. https://doi.org/10.1038/ncb2897.
7. Thompson, S.L., Bakhoum, S.F., and Compton, D.A. (2010). Mechanisms of chromosomal instability. Curr. Biol. *20*, R285–R295, S0960-9822(10)00076-X [pii]. https://doi.org/10.1016/j.cub.2010.01.034.
8. Bastians, H. (2015). Causes of Chromosomal Instability. Recent results in cancer research. Fortschritte der Krebsforschung. Recent Results Cancer Res. *200*, 95–113. https://doi.org/10.1007/978-3-319-20291-4_5.
9. Gregan, J., Polakova, S., Zhang, L., Tolić-Nørrelykke, I.M., and Cimini, D. (2011). Merotelic kinetochore attachment: causes and effects. Trends Cell Biol. *21*, 374–381. https://doi.org/10.1016/j.tcb.2011.01.003.
10. Ertych, N., Stolz, A., Stenzinger, A., Weichert, W., Kaulfuss, S., Burfeind, P., Aigner, A., Wordeman, L., and Bastians, H. (2014). Increased microtubule assembly rates influence chromosomal instability in colorectal cancer cells. Nat. Cell Biol. *16*, 779–791. https://doi.org/10.1038/ncb2994.
11. Bakhoum, S.F., Genovese, G., and Compton, D.A. (2009). Deviant kinetochore microtubule dynamics underlie chromosomal instability. Curr. Biol. *19*, 1937–1942. https://doi.org/10.1016/j.cub.2009.09.055.
12. Ertych, N., Stolz, A., Valerius, O., Braus, G.H., and Bastians, H. (2016). CHK2-BRCA1 tumor-suppressor axis restrains oncogenic Aurora-A kinase to ensure proper mitotic microtubule assembly. Proc. Natl. Acad. Sci. USA. *113*, 1817–1822. https://doi.org/10.1073/pnas.1525129113.
13. Schmidt, A.K., Pudelko, K., Boekenkamp, J.E., Berger, K., Kschischo, M., and Bastians, H. (2021). The p53/p73 - p21(CIP1) tumor suppressor axis guards against chromosomal instability by restraining CDK1 in human cancer cells. Oncogene *40*, 436–451. https://doi.org/10.1038/s41388-020-01524-4.
14. Lüddecke, S., Ertych, N., Stenzinger, A., Weichert, W., Beissbarth, T., Dyczkowski, J., Gaedcke, J., Valerius, O., Braus, G.H., Kschischo, M., and Bastians, H. (2016). The putative oncogene CEP72 inhibits the mitotic function of BRCA1 and induces chromosomal instability. Oncogene *35*, 2398–2406. https://doi.org/10.1038/onc.2015.290.
15. Tamura, N., Shaikh, N., Muliaditan, D., Soliman, T.N., McGuinness, J.R., Maniati, E., Moralli, D., Durin, M.A., Green, C.M., Balkwill, F.R., et al. (2020). Specific mechanisms of chromosomal instability indicate therapeutic sensitivities in high-grade serous ovarian carcinoma. Cancer Res. *80*, 4946–4959. https://doi.org/10.1158/0008-5472.CAN-19-0852.
16. Burrell, R.A., McClelland, S.E., Endesfelder, D., Groth, P., Weller, M.C., Shaikh, N., Domingo, E., Kanu, N., Dewhurst, S.M., Gronroos, E., et al. (2013). Replication stress links structural and numerical cancer chromosomal instability. Nature *494*, 492–496. https://doi.org/10.1038/nature11935.
17. Böhly, N., Kistner, M., and Bastians, H. (2019). Mild replication stress causes aneuploidy by deregulating microtubule dynamics in mitosis. Cell Cycle *18*, 2770–2783. https://doi.org/10.1080/15384101.2019.1658477.
18. Wilhelm, T., Olziersky, A.M., Harry, D., De Sousa, F., Vassal, H., Eskat, A., and Meraldi, P. (2019). Mild replication stress causes chromosome mis-segregation via premature centriole disengagement. Nat. Commun. *10*, 3585. https://doi.org/10.1038/s41467-019-11584-0.
19. Spruck, C.H., Won, K.A., and Reed, S.I. (1999). Deregulated cyclin E induces chromosome instability. Nature *401*, 297–300. https://doi.org/10.1038/45836.
20. Jones, R.M., Mortusewicz, O., Afzal, I., Lorvellec, M., García, P., Helleday, T., and Petermann, E. (2013). Increased replication initiation and conflicts with transcription underlie Cyclin E-induced replication stress. Oncogene *32*, 3744–3753. https://doi.org/10.1038/onc.2012.387.
21. Aziz, K., Limzerwala, J.F., Sturmlechner, I., Hurley, E., Zhang, C., Jeganathan, K.B., Nelson, G., Bronk, S., Fierro Velasco, R.O., van Deursen, E.J., et al. (2019). Ccne1 overexpression causes chromosome instability in liver cells and liver tumor development in mice. Gastroenterology *157*, 210–226.e12. https://doi.org/10.1053/j.gastro.2019.03.016.
22. Macheret, M., and Halazonetis, T.D. (2018). Intragenic origins due to short G1 phases underlie oncogene-induced DNA replication stress. Nature *555*, 112–116. https://doi.org/10.1038/nature25507.
23. Dungrawala, H., Rose, K.L., Bhat, K.P., Mohni, K.N., Glick, G.G., Couch, F.B., and Cortez, D. (2015). The replication checkpoint prevents two types of fork collapse without regulating replisome stability. Mol. Cell *59*, 998–1010. https://doi.org/10.1016/j.molcel.2015.07.030.
24. Simoneau, A., and Zou, L. (2021). An extending ATR-CHK1 circuitry: the replication stress response and beyond. Curr. Opin. Genet. Dev. *71*, 92–98. https://doi.org/10.1016/j.gde.2021.07.003.
25. Santocanale, C., and Diffley, J.F. (1998). A Mec1- and Rad53-dependent checkpoint controls late-firing origins of DNA replication. Nature *395*, 615–618. https://doi.org/10.1038/27001.
26. Paulovich, A.G., and Hartwell, L.H. (1995). A checkpoint regulates the rate of progression through S phase in S. cerevisiae in response to DNA damage. Cell *82*, 841–847. https://doi.org/10.1016/0092-8674(95)90481-6.
27. Forey, R., Poveda, A., Sharma, S., Barthe, A., Padioleau, I., Renard, C., Lambert, R., Skrzypczak, M., Ginalski, K., Lengronne, A., et al. (2020).

Mec1 is activated at the onset of normal S phase by low-dNTP pools impeding DNA replication. Mol. Cell *78*, 396–410.e4. https://doi.org/10.1016/j.molcel.2020.02.021.

28. Johnson, M.C., Can, G., Santos, M.M., Alexander, D., and Zegerman, P. (2021). Checkpoint inhibition of origin firing prevents inappropriate replication outside of S-phase. Elife *10*, e63589. https://doi.org/10.7554/eLife.63589.
29. Fragkos, M., and Naim, V. (2017). Rescue from replication stress during mitosis. Cell Cycle *16*, 613–633. https://doi.org/10.1080/15384101.2017.1288322.
30. Liu, Y., Nielsen, C.F., Yao, Q., and Hickson, I.D. (2014). The origins and processing of ultra fine anaphase DNA bridges. Curr. Opin. Genet. Dev. *26*, 1–5. https://doi.org/10.1016/j.gde.2014.03.003.
31. Bell, S.P., and Labib, K. (2016). Chromosome duplication in Saccharomyces cerevisiae. Genetics *203*, 1027–1067. https://doi.org/10.1534/genetics.115.186452.
32. Moiseeva, T.N., and Bakkenist, C.J. (2018). Regulation of the initiation of DNA replication in human cells. DNA Repair *72*, 99–106. https://doi.org/10.1016/j.dnarep.2018.09.003.
33. Fragkos, M., Ganier, O., Coulombe, P., and Méchali, M. (2015). DNA replication origin activation in space and time. Nat. Rev. Mol. Cell Biol. *16*, 360–374. https://doi.org/10.1038/nrm4002.
34. Costa, A., Ilves, I., Tamberg, N., Petojevic, T., Nogales, E., Botchan, M.R., and Berger, J.M. (2011). The structural basis for MCM2-7 helicase activation by GINS and Cdc45. Nat. Struct. Mol. Biol. *18*, 471–477. https://doi.org/10.1038/nsmb.2004.
35. Moiseeva, T.N., and Bakkenist, C.J. (2019). Dormant origin signaling during unperturbed replication. DNA Repair *81*, 102655. https://doi.org/10.1016/j.dnarep.2019.102655.
36. Ibarra, A., Schwob, E., and Méndez, J. (2008). Excess MCM proteins protect human cells from replicative stress by licensing backup origins of replication. Proc. Natl. Acad. Sci. USA. *105*, 8956–8961. https://doi.org/10.1073/pnas.0803978105.
37. Ge, X.Q., Jackson, D.A., and Blow, J.J. (2007). Dormant origins licensed by excess Mcm2-7 are required for human cells to survive replicative stress. Genes Dev. *21*, 3331–3341. https://doi.org/10.1101/gad.457807.
38. Woodward, A.M., Göhler, T., Luciani, M.G., Oehlmann, M., Ge, X., Gartner, A., Jackson, D.A., and Blow, J.J. (2006). Excess Mcm2-7 license dormant origins of replication that can be used under conditions of replicative stress. J. Cell Biol. *173*, 673–683. https://doi.org/10.1083/jcb.200602108.
39. Lopez-Mosqueda, J., Maas, N.L., Jonsson, Z.O., Defazio-Eli, L.G., Wohlschlegel, J., and Toczyski, D.P. (2010). Damage-induced phosphorylation of Sld3 is important to block late origin firing. Nature *467*, 479–483. https://doi.org/10.1038/nature09377.
40. Zegerman, P., and Diffley, J.F.X. (2010). Checkpoint-dependent inhibition of DNA replication initiation by Sld3 and Dbf4 phosphorylation. Nature *467*, 474–478. https://doi.org/10.1038/nature09373.
41. Abd Wahab, S., and Remus, D. (2020). Antagonistic control of DDK binding to licensed replication origins by Mcm2 and Rad53. Elife *9*, e58571. https://doi.org/10.7554/eLife.58571.
42. Paciotti, V., Clerici, M., Scotti, M., Lucchini, G., and Longhese, M.P. (2001). Characterization of mec1 kinase-deficient mutants and of new hypomorphic mec1 alleles impairing subsets of the DNA damage response pathway. Mol. Cell Biol. *21*, 3913–3925. https://doi.org/10.1128/MCB.21.12.3913-3925.2001.
43. Tercero, J.A., Longhese, M.P., and Diffley, J.F.X. (2003). A central role for DNA replication forks in checkpoint activation and response. Mol. Cell *11*, 1323–1336. https://doi.org/10.1016/s1097-2765(03)00169-2.
44. Moiseeva, T., Hood, B., Schamus, S., O'Connor, M.J., Conrads, T.P., and Bakkenist, C.J. (2017). ATR kinase inhibition induces unscheduled origin firing through a Cdc7-dependent association between GINS and And-1. Nat. Commun. *8*, 1392. https://doi.org/10.1038/s41467-017-01401-x.
45. Petermann, E., Woodcock, M., and Helleday, T. (2010). Chk1 promotes replication fork progression by controlling replication initiation. Proc. Natl. Acad. Sci. USA. *107*, 16090–16095. https://doi.org/10.1073/pnas.1005031107.
46. Shechter, D., Costanzo, V., and Gautier, J. (2004). ATR and ATM regulate the timing of DNA replication origin firing. Nat. Cell Biol. *6*, 648–655. https://doi.org/10.1038/ncb1145.
47. Toledo, L.I., Altmeyer, M., Rask, M.B., Lukas, C., Larsen, D.H., Povlsen, L.K., Bekker-Jensen, S., Mailand, N., Bartek, J., and Lukas, J. (2013). ATR prohibits replication catastrophe by preventing global exhaustion of RPA. Cell *155*, 1088–1103. https://doi.org/10.1016/j.cell.2013.10.043.
48. Moiseeva, T.N., Yin, Y., Calderon, M.J., Qian, C., Schamus-Haynes, S., Sugitani, N., Osmanbeyoglu, H.U., Rothenberg, E., Watkins, S.C., and Bakkenist, C.J. (2019). An ATR and CHK1 kinase signaling mechanism that limits origin firing during unperturbed DNA replication. Proc. Natl. Acad. Sci. USA. *116*, 13374–13383. https://doi.org/10.1073/pnas.1903418116.
49. Moiseeva, T.N., Qian, C., Sugitani, N., Osmanbeyoglu, H.U., and Bakkenist, C.J. (2019). WEE1 kinase inhibitor AZD1775 induces CDK1 kinase-dependent origin firing in unperturbed G1- and S-phase cells. Proc. Natl. Acad. Sci. USA. *116*, 23891–23893. https://doi.org/10.1073/pnas.1915108116.
50. Alver, R.C., Chadha, G.S., Gillespie, P.J., and Blow, J.J. (2017). Reversal of DDK-mediated MCM phosphorylation by Rif1-PP1 regulates replication initiation and replisome stability independently of ATR/Chk1. Cell Rep. *18*, 2508–2520. https://doi.org/10.1016/j.celrep.2017.02.042.
51. Zhang, X., and Kschischo, M. (2022). Distinct and common features of numerical and structural chromosomal instability across different cancer types. Cancers *14*, 1424. https://doi.org/10.3390/cancers14061424.
52. Endesfelder, D., Burrell, R., Kanu, N., McGranahan, N., Howell, M., Parker, P.J., Downward, J., Swanton, C., and Kschischo, M. (2014). Chromosomal instability selects gene copy-number variants encoding core regulators of proliferation in ER+ breast cancer. Cancer Res. *74*, 4853–4863. https://doi.org/10.1158/0008-5472.CAN-13-2664.
53. Carter, S.L., Eklund, A.C., Kohane, I.S., Harris, L.N., and Szallasi, Z. (2006). A signature of chromosomal instability inferred from gene expression profiles predicts clinical outcome in multiple human cancers. Nat. Genet. *38*, 1043–1048.
54. Diener, C., and Resendis-Antonio, O. (2016). Personalized prediction of proliferation rates and metabolic liabilities in cancer biopsies. Front. Physiol. *7*, 644. https://doi.org/10.3389/fphys.2016.00644.
55. Akerman, I., Kasaai, B., Bazarova, A., Sang, P.B., Peiffer, I., Artufel, M., Derelle, R., Smith, G., Rodriguez-Martinez, M., Romano, M., et al. (2020). A predictable conserved DNA base composition signature defines human core DNA replication origins. Nat. Commun. *11*, 4826. https://doi.org/10.1038/s41467-020-18527-0.
56. Naim, V., and Rosselli, F. (2009). The FANC pathway and BLM collaborate during mitosis to prevent micro-nucleation and chromosome abnormalities. Nat. Cell Biol. *11*, 761–768. https://doi.org/10.1038/ncb1883.
57. Rodriguez-Acebes, S., Mourón, S., and Méndez, J. (2018). Uncoupling fork speed and origin activity to identify the primary cause of replicative stress phenotypes. J. Biol. Chem. *293*, 12855–12861. https://doi.org/10.1074/jbc.RA118.003740.
58. Koltun, E.S., Tsuhako, A.L., Brown, D.S., Aay, N., Arcalas, A., Chan, V., Du, H., Engst, S., Ferguson, K., Franzini, M., et al. (2012). Discovery of XL413, a potent and selective CDC7 inhibitor. Bioorg. Med. Chem. Lett. *22*, 3727–3731. https://doi.org/10.1016/j.bmcl.2012.04.024.
59. Zhong, Y., Nellimoottil, T., Peace, J.M., Knott, S.R.V., Villwock, S.K., Yee, J.M., Jancuska, J.M., Rege, S., Tecklenburg, M., Sclafani, R.A., et al. (2013). The level of origin firing inversely affects the rate of replication fork progression. J. Cell Biol. *201*, 373–383. https://doi.org/10.1083/jcb.201208060.
60. Brouhard, G.J., Stear, J.H., Noetzel, T.L., Al-Bassam, J., Kinoshita, K., Harrison, S.C., Howard, J., and Hyman, A.A. (2008). XMAP215 is a processive microtubule polymerase. Cell *132*, 79–88. https://doi.org/10.1016/j.cell.2007.11.043.

61. Hirai, H., Iwasawa, Y., Okada, M., Arai, T., Nishibata, T., Kobayashi, M., Kimura, T., Kaneko, N., Ohtani, J., Yamanaka, K., et al. (2009). Small-molecule inhibition of Wee1 kinase by MK-1775 selectively sensitizes p53-deficient tumor cells to DNA-damaging agents. Mol. Cancer Ther. *8*, 2992–3000. https://doi.org/10.1158/1535-7163.MCT-09-0463.

62. Beck, H., Nähse-Kumpf, V., Larsen, M.S.Y., O'Hanlon, K.A., Patzke, S., Holmberg, C., Mejlvang, J., Groth, A., Nielsen, O., Syljuåsen, R.G., and Sørensen, C.S. (2012). Cyclin-dependent kinase suppression by WEE1 kinase protects the genome through control of replication initiation and nucleotide consumption. Mol. Cell Biol. *32*, 4226–4236. https://doi.org/10.1128/MCB.00412-12.

63. Shima, N., and Pederson, K.D. (2017). Dormant origins as a built-in safeguard in eukaryotic DNA replication against genome instability and disease development. DNA Repair *56*, 166–173. https://doi.org/10.1016/j.dnarep.2017.06.019.

64. Boos, D., and Ferreira, P. (2019). Origin firing regulations to control genome replication timing. Genes *10*, 199. https://doi.org/10.3390/genes10030199.

65. Sillars-Hardebol, A.H., Carvalho, B., Tijssen, M., Beliën, J.A.M., de Wit, M., Delis-van Diemen, P.M., Pontén, F., van de Wiel, M.A., Fijneman, R.J.A., and Meijer, G.A. (2012). TPX2 and AURKA promote 20q amplicon-driven colorectal adenoma to carcinoma progression. Gut *61*, 1568–1575. https://doi.org/10.1136/gutjnl-2011-301153.

66. Li, H., Cao, Y., Ma, J., Luo, L., and Ma, B. (2021). Expression and prognosis analysis of GINS subunits in human breast cancer. Medicine (Baltim.) *100*, e24827. https://doi.org/10.1097/MD.0000000000024827.

67. He, Z., Wang, X., Yang, Z., Jiang, Y., Li, L., Wang, X., Song, Z., Wang, X., Wan, J., Jiang, S., et al. (2021). Expression and prognosis of CDC45 in cervical cancer based on the GEO database. PeerJ *9*, e12114. https://doi.org/10.7717/peerj.12114.

68. Littler, S., Sloss, O., Geary, B., Pierce, A., Whetton, A.D., and Taylor, S.S. (2019). Oncogenic MYC amplifies mitotic perturbations. Open Biol. *9*, 190136. https://doi.org/10.1098/rsob.190136.

69. Caldon, C.E., Sergio, C.M., Burgess, A., Deans, A.J., Sutherland, R.L., and Musgrove, E.A. (2013). Cyclin E2 induces genomic instability by mechanisms distinct from cyclin E1. Cell Cycle *12*, 606–617. https://doi.org/10.4161/cc.23512.

70. Irony-Tur Sinai, M., and Kerem, B. (2018). DNA replication stress drives fragile site instability. Mutat. Res. *808*, 56–61. https://doi.org/10.1016/j.mrfmmm.2017.10.002.

71. Letessier, A., Millot, G.A., Koundrioukoff, S., Lachagès, A.M., Vogt, N., Hansen, R.S., Malfoy, B., Brison, O., and Debatisse, M. (2011). Cell-type-specific replication initiation programs set fragility of the FRA3B fragile site. Nature *470*, 120–123. https://doi.org/10.1038/nature09745.

72. Barlow, J.H., Faryabi, R.B., Callén, E., Wong, N., Malhowski, A., Chen, H.T., Gutierrez-Cruz, G., Sun, H.W., McKinnon, P., Wright, G., et al. (2013). Identification of early replicating fragile sites that contribute to genome instability. Cell *152*, 620–632. https://doi.org/10.1016/j.cell.2013.01.006.

73. St Germain, C., Zhao, H., and Barlow, J.H. (2021). Transcription-replication collisions-A series of Unfortunate events. Biomolecules *11*, 1249. https://doi.org/10.3390/biom11081249.

74. Kabeche, L., Nguyen, H.D., Buisson, R., and Zou, L. (2018). A mitosis-specific and R loop-driven ATR pathway promotes faithful chromosome segregation. Science *359*, 108–114. https://doi.org/10.1126/science.aan6490.

75. Hengeveld, R.C.C., de Boer, H.R., Schoonen, P.M., de Vries, E.G.E., Lens, S.M.A., and van Vugt, M.A.T.M. (2015). Rif1 is required for resolution of Ultrafine DNA bridges in anaphase to ensure genomic stability. Dev. Cell *34*, 466–474. https://doi.org/10.1016/j.devcel.2015.06.014.

76. Cimini, D., Howell, B., Maddox, P., Khodjakov, A., Degrassi, F., and Salmon, E.D. (2001). Merotelic kinetochore orientation is a major mechanism of aneuploidy in mitotic mammalian tissue cells. J. Cell Biol. *153*, 517–527.

77. Galjart, N. (2010). Plus-end-tracking proteins and their interactions at microtubule ends. Curr. Biol. *20*, R528–R537. https://doi.org/10.1016/j.cub.2010.05.022.

78. Yu, J.X., Chen, Q., Yu, Y.Q., Li, S.Q., and Song, J.F. (2016). Upregulation of colonic and hepatic tumor overexpressed gene is significantly associated with the unfavorable prognosis marker of human hepatocellular carcinoma. Am. J. Cancer Res. *6*, 690–700.

79. Charrasse, S., Mazel, M., Taviaux, S., Berta, P., Chow, T., and Larroque, C. (1995). Characterization of the cDNA and pattern of expression of a new gene over-expressed in human hepatomas and colonic tumors. Eur. J. Biochem. *234*, 406–413.

80. Silkworth, W.T., and Cimini, D. (2012). Transient defects of mitotic spindle geometry and chromosome segregation errors. Cell Div. *7*, 19. https://doi.org/10.1186/1747-1028-7-19.

81. Köhler, C., Koalick, D., Fabricius, A., Parplys, A.C., Borgmann, K., Pospiech, H., and Grosse, F. (2016). Cdc45 is limiting for replication initiation in humans. Cell Cycle *15*, 974–985. https://doi.org/10.1080/15384101.2016.1152424.

82. Seibert, M., Krüger, M., Watson, N.A., Sen, O., Daum, J.R., Slotman, J.A., Braun, T., Houtsmuller, A.B., Gorbsky, G.J., Jacob, R., et al. (2019). CDK1-mediated phosphorylation at H2B serine 6 is required for mitotic chromosome segregation. J. Cell Biol. *218*, 1164–1181. https://doi.org/10.1083/jcb.201806057.

83. Stepanova, T., Slemmer, J., Hoogenraad, C.C., Lansbergen, G., Dortland, B., De Zeeuw, C.I., Grosveld, F., van Cappellen, G., Akhmanova, A., and Galjart, N. (2003). Visualization of microtubule growth in cultured neurons via the use of EB3-GFP (end-binding protein 3-green fluorescent protein). J. Neurosci. *23*, 2655–2664.

84. Ferreira, P., Sanchez-Pulido, L., Marko, A., Ponting, C.P., and Boos, D. (2022). Refining the domain architecture model of the replication origin firing factor Treslin/TICRR. Life Sci. Alliance *5*, e202101088. https://doi.org/10.26508/lsa.202101088.

85. Carter, S.L., Cibulskis, K., Helman, E., McKenna, A., Shen, H., Zack, T., Laird, P.W., Onofrio, R.C., Winckler, W., Weir, B.A., et al. (2012). Absolute quantification of somatic DNA alterations in human cancer. Nat. Biotechnol. *30*, 413–421. https://doi.org/10.1038/nbt.2203.

86. Cancer Genome Atlas Research Network; Weinstein, J.N., Collisson, E.A., Mills, G.B., Shaw, K.R.M., Ozenberger, B.A., Ellrott, K., Shmulevich, I., Sander, C., and Stuart, J.M. (2013). The cancer genome Atlas pan-cancer analysis project. Nat. Genet. *45*, 1113–1120. https://doi.org/10.1038/ng.2764.

87. Viechtbauer, W. (2010). Conducting meta-analyses in R with the metafor package. J. Stat. Softw. *36*, 1–48.

88. Hahsler, M., Grün, B., and Hornik, K. (2005). Arules - a computational environment for mining association Rules and frequent item sets. J. Stat. Softw. *14*. https://doi.org/10.18637/jss.v18014.i18615.

89. Subramanian, A., Tamayo, P., Mootha, V.K., Mukherjee, S., Ebert, B.L., Gillette, M.A., Paulovich, A., Pomeroy, S.L., Golub, T.R., Lander, E.S., and Mesirov, J.P. (2005). Gene set enrichment analysis: a knowledge-based approach for interpreting genome-wide expression profiles. Proc. Natl. Acad. Sci. USA. *102*, 15545–15550. https://doi.org/10.1073/pnas.0506580102.

## STAR★METHODS

### KEY RESOURCES TABLE

| REAGENT or RESOURCE | SOURCE | IDENTIFIER |
|---|---|---|
| Antibodies | | |
| anti-α-tubulin | Santa Cruz | Cat#: Sc-23948; RRID:AB_628410 |
| Aati-CenpC | MBL International | Cat#: PD030: RRID:AB_10693556 |
| anti-FANCD2 antibodies | Novus Biologicals | Cat#: NB100-182SS; RRID:AB_1108397 |
| anti-BrdU (for CldU detection) | Abcam | Cat#: ab6326; RRID:AB_305426 |
| anti-BrdU (for IdU detection; | Beckton Dickson | Cat#: 347580; RRID:AB_10015219 |
| Anti-ssDNA | DSHB | Cat#: Autoanti-ssDNA; RRID:AB_10805144 |
| anti-β-actin | Sigma | Cat#: A5441; RRID:AB_476744 |
| anti-Cdc45 | Cell Signaling | Cat#: 11881S; RRID:AB_2715569 |
| anti-Cdc7 | Abcam | Cat#: ab229187 |
| anti-chTOG | Santa Cruz | Cat#: sc-37439 |
| Anti-Mcm2 | Cell Signaling | Cat#: 3619S; RRID:AB_2142137 |
| anti-Mcm4 | Cell Signaling | Cat#: 3228; RRID:AB_11178393 |
| anti-Mcm6 | Santa Cruz | Cat#: sc-55576; RRID:AB_831539 |
| anti-Psf1 (Gins1) | Abcam | Cat#: ab181112 |
| anti-Psf2 (Gins2) | Proteintech | Cat#: 16247-1-AP; RRID:AB_2111895 |
| Anti-RIF1 | Cell Signaling | Cat#: 95558; RRID:AB_2800249 |
| Anti-MPM2 (FACS) | Merck Millipore | Cat#: 05–368; RRID:AB_309698 |
| Anti-BrdU (FACS) | Beckton Dickson | Cat#: 556028; RRID:AB_396304 |
| Chemicals, peptides, and recombinant proteins | | |
| ATR inhibitor ETP-46464 | Selleck | Cat#: S8050 |
| WEE1 inhibitor MK-1775 | Selleck | Cat#: S1525 |
| CDK1 inhibitor RO-3306 | Santa Cruz | Cat#: sc-1059169 |
| CDC7 inihbitor XL-413 | Tocris | Cat#: 5493 |
| DNA polymerase inhibitor aphidicolin | Santa Cruz | Cat#: sc-201535 |
| Eg5 inhibitor Dimethylenastron | Sigma | Cat#: SML0905 |
| Taxol | Sigma | Cat#: T7191 |
| Experimental models: Cell lines | | |
| HCT116 | ATCC | Cat#: CCL-247; RRID:CVCL_0291 |
| HT29 | ATCC | Cat#: HTB-38; RRID:CVCL_0320 |
| SW480 | ATCC | Cat#: CCL-228; RRID:CVCL_0546 |
| SW620 | ATCC | Cat#: CCL-227; RRID:CVCL_0547 |
| RPE1-hTert | gift from Dr. Uwe Wolfrum, University of Mainz, Germany | |
| HCT116 + *CDK1-AF* | Schmidt et al.[13] | |
| HCT116 + *GINS1* | This manuscript | |
| HCT116 + *CDC45* | This manuscript | |
| Oligonucleotides | | |
| Luciferase siRNA: 5′-CUUACGCUGAGUACUUCGAUU-3′ | Sigma | custom made |
| *CDC45 siRNA*: 5′-UUCAUCCAGGCUCUGGACAGC-3′ | Sigma | custom made |
| *CDC7 siRNA*: 5′-AAGCUCAGCAGGAAAGGUG-3′ | Sigma | custom made |

(*Continued on next page*)

*Continued*

| REAGENT or RESOURCE | SOURCE | IDENTIFIER |
|---|---|---|
| *GINS1 siRNA* : 5′-AAAGAUCUCUUGCUACUUA-3′ | Sigma | custom made |
| *MCM2 siRNA*: 5′GGAGCUCAUUG GAGAUGGCAUGGAA-3′ | Sigma | custom made |
| *RIF1*: 5′-AAGAGCAUCUCAGGGUUUGCU-3′ | Sigma | custom made |
| **Recombinant DNA** | | |
| pEGFP-*EB3* | gift from Dr. Linda Wordeman, Seattle, WA, USA | |
| pCMV6-Myc-FLAG-*GINS1* | OriGene Technologies, Inc., USA | Cat#: RC203049 |
| mCherry-*CDC45* | Kohler et al.[81] | |
| pcDNA 3.1 | Invitrogen | Cat#: V79020 |
| **Software and algorithms** | | |
| Microscopy software SoftWoRx® Software Suite | GE Healthcare | Version 6.0 |
| GraphPad Prism | GraphPad Software | Version 5 |
| **Other** | | |
| RPMI culture medium | PAB Biotech | Cat#: P04-16500 |
| DMEM-F12 culture medium | PAN Biotech | Cat#: P04-41500 |
| fetal calf serum (FBS) | Corning | Cat#:15377636 |
| Penicillin/Streptomycin | Anprotec | Cat#: AC-AB-0024 |
| G418 | Santa Cruz | Cat#: sc-29065B |

## RESOURCE AVAILABILITY

### Lead contact

Further information and requests for resources and reagents should be directed to and will be fulfilled by the lead contact, Holger Bastians (holger.bastians@uni-goettingen.de).

### Materials availability

Cell lines generated in this study are available upon requires with the restriction to accept regulations defined in an MTA.

### Data and code availability

- All data reported in this paper will be shared by the lead contact upon request.
- This paper does not report original code.
- Any additional information required to reanalyze the data reported in this paper is available from the lead contact upon request.

## EXPERIMENTAL MODEL AND SUBJECT DETAILS

### Mammalian cell lies and growth conditions

HCT116, HT29, SW480, and SW620 cells were obtained from ATCC (USA, see key resources table). Cells were cultivated in RPMI1640 medium (PAN-Biotech GmbH, Germany) supplemented with 10% fetal bovine serum (FBS; Corning Inc., USA), 100 units/mL penicillin, and 100 μg/mL streptomycin (Anprotec, Germany). HCT116 + *CDK1-AF* and the corresponding control cells[13] were grown in medium with 300 μg/mL G418 (Santa Cruz, USA). RPE-1-hTert cells were cultivated in DMEM-F12 supplemented with 10% fetal bovine serum (FBS; Corning Inc., USA), 100 units/mL penicillin, and 100 μg/mL streptomycin (Anprotec, Germany) and 0,26% $NaHCO_3$. All cells were grown in a humidified atmosphere at 37°C and 5% $CO_2$.

### Generation of stable cell lines

For the generation of HCT116-derived cell lines stably expressing *CDC45* or *GINS1*, HCT116 cells were transfected with 0.75 μg mCherry-*CDC45* (kindly provided by Helmut Pospiech, FLI, Jena, Germany[81]) or 1.5 μg pCMV6-Myc-FLAG-*GINS1* (OriGene Technologies, Inc., USA) or with 1.5 μg pcDNA3.1 (Invitrogen, USA) using METAFECTENE (Biontex, Germany) according to the manufacturer instructions. Several single cell clones were grown in medium supplemented with 300 μg/mL G418 (Santa Cruz, USA) and

selected for further analysis. HCT116 cells stably expressing CDK1-AF were described before[13] using pcDNA3-Flag-CDK1-AF (kindly provided by Makoto Iimori, Kyushu, Japan and Lienhard Schmitz, Giessen, Germany).[82]

## METHOD DETAILS

### Plasmid and siRNA transfections

For EB3-GFP tracking experiments, cells were transfected with 10 μg pEGFP-*EB3* (kindly provided by Linda Wordeman, Seattle, WA, USA) using a GenePulser Xcell (Bio-Rad Laboratories, USA) at 500 μF and 300 V (HCT116, SW620), or 950 μF and 220 V (SW480, HT29). RPE-1 cells were transfected with plasmids expressing *GINS1* (pCMV6-Myc-FLAG-*GINS1)* or *CDC45* (mCherry-*CDC45)* (kindly provided by Helmut Pospiech, FLI, Jena, Germany[81]) using Lipofectamin 3000 (Thermo Fisher Scientific, USA) according to the manufacturer protocols. Cells were transfected with siRNAs (30–90 pmol; Sigma-Aldrich, Germany) using ScreenFect®siRNA (ScreenFect GmbH, Germany) or Lipofectamine RNAiMAX (Thermo Fisher Scientific, USA) according to the manufacturer protocols. The used siRNA sequences (Sigma, custom made) are listed in the key resources table. Further experiments were performed 48 hrs after transfection and Western blotting was used to confirm transfection efficiency.

### Cell treatments

To restore proper microtubule polymerization rates, cells were grown in the presence of 0.2 nM Taxol (Sigma, Germany) as shown before.[10,12] The inhibitors ETP-46464 (1.0 μM; Selleck Chemicals, USA), MK-1775 (75 nM; Selleck Chemicals, USA), RO-3306 (1.0 μM; Santa Cruz, USA), and XL-413 (0.5–1.0 μM; Tocris Bioscience, UK) were used to inhibit ATR, Wee1, CDK1, and Cdc7 kinases, respectively. All inhibitors were titrated to ensure that cell cycle progression was not affected. Cells were treated with 100–400 nM aphidicolin (Santa Cruz, USA) to induce mild replication stress as described before.[17] Corresponding volumes of DMSO or $H_2O$ were used as controls.

### Analysis of microtubule polymerization rates

EB3-GFP tracking experiments were performed to determine microtubule polymerization rates.[10,83] 48–72 hrs after transfection with pEGFP-*EB3*, cells were treated with 2.0 μM Dimethylenastron (DME; Sigma, Germany) for 1–2 hrs to accumulate cells in prometaphase.[10] This synchronization step ensured that microtubule growth was determined in the same mitotic stage in each experiment. DME treatment did not affect microtubule growth rates per se.[10] To visualize microtubule plus tips, live cell microscopy was performed using a DeltaVision Elite microscope (GE Healthcare, UK) equipped with a PCO Edge sCMOS camera (PCO, Germany) and the softWoRx® 6.0 Software Suite (GE Healthcare, USA). Mitotic cells were monitored for 30 seconds in total, and images were taken every 2 seconds. During image acquisition, cells were incubated at 37°C and 5% $CO_2$. The softWoRx® 6.0 Software Suite (GE Healthcare, USA) was used for image deconvolution and analysis. Average microtubule growth rates were calculated from 20 microtubules per cell.

### Quantification of anaphase cells exhibiting lagging chromosomes

Cells were synchronized in anaphase by a double thymidine block followed by a release for 8.5–9.5 hrs to enrich anaphase cells used for immunofluorescence miscroscopy detecting lagging chromosomes.[13] For detection of lagging chromosomes in RPE-1 cells, a single thymidine block and release for 9 hours was used to enrich cells in anaphase. Cells were fixed with 2% paraformaldehyde/PBS for 5 minutes and then with ice-cold 100% methanol for 5 minutes at −20°C. To visualize microtubules, kinetochores, and the DNA, cells were stained with anti-α-tubulin (1:700, B-5-1-2, Santa Cruz, USA, cat no sc-23948), anti-CENP-C (1:1000, MBL International Corporation, USA, cat no PD030) and secondary antibodies conjugated to Alexa488 (1:1000, Thermo Fisher Scientific, USA, cat no A-11029) and Alexa594 (1:1000, Thermo Fisher Scientific, USA, cat no A-11076), and Hoechst33342 (1:15000 in PBS, Thermo Fisher Scientific, USA). To quantify cells exhibiting lagging chromosomes, 100 anaphase cells were analyzed in each experiment using a Leica DMI6000B fluorescence microscope (Leica, Germany) equipped with a Leica DFC360 FX camera (Leica, Germany) and the Leica LAS AF software (Leica, Germany). Only Cenp-C positive chromosomes and clearly separated from the bulk of segregated DNA were considered as lagging chromosomes.

### Detection of FANCD2 foci

For the detection of FANCD2 foci in prometaphase cells, cells were fixed with 2% (w/v) paraformaldehyde/PBS for 5 minutes followed by treatment with ice-cold 100% (v/v) methanol for 5 minutes at −20°C. Cells were blocked in 5% (v/v) FBS in PBS for 30 minutes at RT. After washing with PBS staining with anti-FANCD2 antibodies (1:500, Novus Biologicals, USA, cat no NB100-182SS) in 2% (v/v) FBS in PBS was performed for 1.5 hours at room temperature. After 3 washing steps with PBS cells were incubated with secondary antibodies conjugated to Alexa-Fluor488 (1:1000, Thermo Fisher Scientific, USA, cat no A-11029) for 1 hour at RT. Subsequently, DNA was stained with Hoechst33342 (1:15,000 in PBS, Thermo Fisher Scientific, USA) for 5 min at RT. Finally cells were washed four times with PBS, dried and mounted onto glass slides with VectaShield (H-1000, Vector Laboratories, Germany). Imaging was performed with a Leica DMI6000B fluorescence microscope (Leica, Germany) equipped with a Leica DFC360 FX camera (Leica, Germany) and the Leica LAS AF software (Leica, Germany).

### Detection of W-CIN and gross structural aberrations

To assess time-dependent W-CIN, we analyzed the generation of aneuploidy in single cell clones that were grown for 30 generations in culture. Cells were subjected to chromosome counting analysis from metaphase spreads as described.[10,13] Briefly, cells were treated for 4 hrs with 2.0 μM of the Eg5 inhibitor Dimethylenanstron (DME) for 4 hrs to accumulate cells in mitosis. Cells were harvested and resuspended in hypotonic solution (60% $ddH_2O$ + 40% RPMI6140 (PAN-Biotech GmbH, Germany)). After 15 minutes of incubation at room temperature, cells were fixed with ice-cold 75% methanol +25% acetic acid. After fixation, cells were resuspended in 100% acetic acid and dropped onto pre-cooled wet glass slides. After drying, cells were stained with Giemsa solution (Sigma-Aldrich, Germany). The chromosome number of 50 mitotic cells was quantified using a Zeiss Axioscope FS microscope (Zeiss, Germany) equipped with a Hamamatsu digital camera C4742-95 (Hamamatsu Photonics, Japan) and the Hokawo Launcher 2.1 software (Hamamatsu Photonics, Japan). Chromosome spreads were also analyzed for the presence of visible chromosome aberrations (e.g. breaks, fusions).

### DNA combing assays

DNA combing assays were performed to determine DNA replication fork progression rates and inter-origin distances. Asynchronously growing cells were pre-treated with inhibitors as indicated for the specific experiments (aphidicolin, ETP-46464, RO-3306, XL-413) for 1 h followed by inhibitor incubation together with 100 μM 5-chloro-2'-deoxyuridine (CldU; Sigma-Aldrich, Germany) and, subsequently, with 100 μM 5-iodo-2'-deoxyuridine (IdU; Sigma-Aldrich, Germany) for 30 min each. Cells were harvested and processed using the FiberPrep DNA extraction kit (Genomic Vision, France). Isolated DNA was immobilized on engraved vinyl silane treated cover slips (Genomic Vision, France) using the Molecular Combing System (Genomic Vision, France). Subsequently, samples were stained with the following antibodies: anti-BrdU (for CldU detection; 1:10, BU1/75 (ICR1), Abcam, UK, cat no ab6326), anti-BrdU (for IdU detection; 1:10, B44, BD Biosciences, USA, cat no 347580), anti-ssDNA (1:5, DSHB, USA, cat no autoanti-ssDNA), secondary antibodies conjugated to Cy5 (1:25, Abcam, UK, cat no ab6565), Cy3.5 (1:25, Abcam, UK, cat no ab6946), and BV480 (1:25, BD Biosciences, USA, cat no 564877). Images were acquired by Genomic Vision's EasyScan service and samples were analyzed with the FiberStudio web application (Genomic Vision, France). To determine replication fork progression rates, at least 300 labeled unidirectional DNA tracks were analyzed per sample. To analyze inter-origin distances, the distance between two neighboring origins on the same DNA strand was measured. At least 45 inter-origin distances were analyzed per sample.

### Western blotting

Cells were lysed in lysis buffer (50 mM Tris-HCl, pH 7.4, 150 mM NaCl, 5 mM EDTA, 5 mM EGTA, 1% (v/v) NP-40, 0.1% (w/v) SDS, 0.1% (w/v) sodium deoxycholate, phosphatase inhibitor cocktail (25 mM β-glycerophosphate, 50 mM NaF, 5 mM $Na_2MoO_4$, 0.2 mM $Na_3VO_4$, 5 mM EDTA, 0.5 μM microcystin), protease inhibitor cocktail (Roche, Switzerland)). After separation on SDS polyacrylamide gels (7%, 11%, or 13%), proteins were blotted onto nitrocellulose membranes. The following antibodies were used in the indicated dilutions: anti-α-tubulin (1:1000, B-5-1-2, Santa Cruz, USA, cat no sc-23948), anti-β-actin (1:10000, AC-15, Sigma-Aldrich, Germany, cat no A5441), anti-Cdc45 (1:1000, D7G6, Cell Signaling Technology, USA, cat no #11881S), anti-Cdc7 (1:1000, EPR20337, Abcam, UK, cat no ab229187), anti-chTOG (H-4, 1:400, Santa Cruz Biotechnology, cat no sc-37439), anti-Mcm2 (1:5000, D7G11, Cell Signaling Technology, USA, cat no #3619S), anti-Mcm4 (1:1000, Cell Signalling Technologies, USA, cat no #3228), anti-Mcm6 (1:1000, B4, Santa Cruz, USA, cat no sc-55576) anti-Psf1 (Gins1) (1:10000, EPR13359, Abcam, UK, cat no ab181112), anti-Psf2 (Gins2) (1:1000, Proteintech, USA, cat no 16247-1-AP), anti-RIF1 (1:1000, D2F2M, Cell Signaling Technology, USA, cat no #95558). Secondary antibodies conjugated to horseradish peroxidase were used in 3% non-fat milk in TBS for 1 hour (1:10000, Jackson ImmunoResearch Laboratories, Inc., USA, cat no 115-035-146, 111-035-144). Proteins were detected by enhanced chemiluminescence.

### Flow cytometry analyses

DNA content was determined using a BD FACS Canto II flow cytometer (Becton Dickinson, USA). For this, cells were harvested, resuspended in 500 μL PBS and fixed in 2 mL 70% ice-cold ethanol and stored overnight at 4°C. Cells were washed in 0.05% TritonX-100/PBS and incubated with RNase A (1 mg/mL in PBS) for 30 min at room temperature. DNA was stained using propidium iodide (1 μg/mL; Carl Roth, Germany). Mitotic cells were stained using anti-MPM-2 antibodies (1:1600; Merck Millipore, USA, cat no 05-368) as described.[10] 5-Bromo-2-desoxyuridin (BrdU) labeling was performed by culturing the cells in the presence of 10 μM BrdU (Carl Roth, Germany, cat no 3243.1). BrdU incorporation was detected using FITC-coupled Anti-BrdU antibodies (clone 3D4; Beckton Dickson Pharmingen, USA, cat no 556028) as described.[84]

### TCGA molecular and ploidy data

Copy number segment data, gene expression profiles and the ploidy status called by the ABSOLUTE algorithm[85] of TCGA primary tumors across 32 cancer types were downloaded from the pan cancer atlas.[86] Analyzed cancer types included: adrenocortical carcinoma (ACC), bladder urothelial carcinoma (BLCA), breast invasive carcinoma (BRCA), cervical and endocervical cancers (CESC), cholangiocarcinoma (CHOL), colon adenocarcinoma (COAD), lymphoid neoplasm diffuse large B-cell lymphoma (DLBC), esophageal carcinoma (ESCA), glioblastoma multiforme (GBM), head and neck squamous cell carcinoma (HNSC), kidney chromophobe (KICH), kidney cancer (KIPAN), kidney renal clear cell carcinoma (KIRC), kidney renal papillary cell carcinoma (KIRP), acute myeloid

leukemia (LAML), brain lower grade glioma (LGG), liver hepatocellular carcinoma (LIHC), lung adenocarcinoma (LUAD), lung squamous cell carcinoma (LUSC), ovarian serous cystadenocarcinoma (OV), pancreatic adenocarcinoma (PAAD), pheochromocytoma and paraganglioma (PCPG), prostate adenocarcinoma (PRAD), rectum adenocarcinoma (READ), sarcoma (SARC), skin cutaneous melanoma (SKCM), stomach adenocarcinoma (STAD), testicular germ cell tumors (TGCT), thyroid carcinoma (THCA), thymoma (THYM), uterine corpus endometrial carcinoma (UCEC), uterine carcinosarcoma (UCS) and uveal melanoma (UVM). A total of 9,573 tumor samples, for which copy number segment data, gene expression profiles and the ploidy status data were available, were used for the analysis. The predicted proliferation rates were collected from.[54]

### Quantifying W-CIN

We computed the numerical complexity score (NCS) as proxy measure of W-CIN. NCS is defined as the number of chromosomes of which at least 75% of the chromosome lengths have copy number gains/losses relative to the sample ploidy.[16] The calculation of NCS for each sample was proceeded by: (1) rounding the segment-wise autosomal copy numbers and the ABSOLUTE[85] inferred ploidy to the nearest integers; (2) counting the number of chromosomes with 75% of the corresponding chromosomal length have higher or lower integer copy numbers relative to the integer ploidy, resulting in the sample NCS.

### Quantifying overall CIN

We computed the weighted genome integrity index (WGII) as the surrogate measure of overall CIN levels. The WGII score is defined as the average percentage of changed genome relative to the sample ploidy over 22 autosomal chromosomes and ranges from zero to one.[16] We calculated the WGII score for each sample by the following steps: (1) rounding the segment-wise autosomal copy numbers and ABSOLUTE inferred ploidy to nearest integers; (2) counting the proportions of segments whose integer copy numbers differ from sample ploidy for 22 autosomes; (3) averaging the proportions of changed segments derived from (2) over all autosomes, resulting in the sample WGII.

### Chromosome instability and gene expression association analysis

We performed gene-wise max-min normalization in each cancer type to transform gene expression values to the range between zero. To categorize the tumor samples of a given cancer type as either low or high NCS (W-CIN), we used a k-means based discretization method implemented in the R package *arules*.[87] To account for cancer type specific effects, we used a meta analysis method implemented in the R package *metafor*.[88] To estimate the meta-mean difference in gene expression between both low and high NCS groups we used the *escalc* and *rma* functions in *metafor* with the setting measure = "MD" and method = "FE". Standard FDR estimates were computed to correct the pvalues for multiple testing. We additionally performed the same analysis replacing NCS with WGII to investigate the relationship between overall CIN and the upregulation of origin firing factors.

### Correcting the confounding effect of proliferation rates

To correct the confounding effect of proliferation rates on the relationship between origin firing gene expression and CIN, we computed the Spearman rank correlation coefficient based partial correlation coefficients (PCC) between CIN scores (NCS/WGII) and gene expression controlling the effect of proliferation rates. The PCC can be obtained from the three pairwise Spearman rank correlation coefficients: $r_{(CIN,gene)}$ $r_{(proliferation,CIN)}$, $r_{(proliferation,gene)}$ as $PCC_{(CIN,gene)|(proliferation)} = \frac{r_{(CIN,gene)} - r_{(proliferation,CIN)} \times r_{(proliferation,gene)}}{\sqrt{(1 - r^2_{(proliferation,CIN)}) \times (1 - r^2_{(proliferation,gene)})}}$.

### Chromosome instability and copy number association analysis

The association between chromosome instability and copy number variations (CNVs) were analyzed as for gene expression analysis, replacing gene expression with copy number.

### Gene set enrichment analysis

We used a manually curated list of origin firing genes (*MCM2*, *MCM3*, *MCM4*, *MCM5*, *MCM6*, *MCM7*, *CDC7*, *DBF4*, *GINS1*, *POLD1*, *POLD2*, *POLD3*, *POLE*, *PCNA*, *GINS2*, *GINS3*, *GINS4*, *CDC45*, *CDK1*, *CCNE1*, *CCNE2*, *CDK2*, *CCNA1*, *CCNA2*, *WDHD1*, *RECQL4*, *TRESLIN*, *TOPBP1*) and KEGG replication factors (https://www.genome.jp/kegg/) as gene sets to perform gene set enrichment analysis (GSEA).[89] All genes were ranked according to the PCC between their expression and NCS controlling proliferation rates. The replication gene or origin firing gene sets were tested for significance enriched at the top of this ranked list.

## QUANTIFICATION AND STATISTICAL ANALYSIS

The GraphPad Prism 5.0 software (GraphPad Software, USA) was used for statistical analysis. Mean values and standard deviation (SD) were calculated. Unpaired two-tailed *t*-tests (SD $\neq$ 0) or one-sample *t*-tests (SD = 0) were applied to analyze statistical significance. All statistical tests used for analysis of specific experiments are indicated in the Figure Legends. p-values were indicated as: ns (not significant): $p \geq 0.05$, *: $p < 0.05$, **: $p < 0.01$, ***: $p < 0.001$, ****: $p < 0.0001$.